



Universiteit
Leiden
The Netherlands

Synthetic tools to study ubiquitin biology

Shahul Hameed, D.A.

Citation

Shahul Hameed, D. A. (2020, June 23). *Synthetic tools to study ubiquitin biology*. Retrieved from <https://hdl.handle.net/1887/123181>

Version: Publisher's Version

License: [Licence agreement concerning inclusion of doctoral thesis in the Institutional Repository of the University of Leiden](#)

Downloaded from: <https://hdl.handle.net/1887/123181>

Note: To cite this publication please use the final published version (if applicable).

Cover Page



Universiteit Leiden



The handle <http://hdl.handle.net/1887/123181> holds various files of this Leiden University dissertation.

Author: Shahul Hameed D.A.

Title: Synthetic tools to study ubiquitin biology

Issue Date: 2020-06-23

Chapter 3

Diubiquitin-based NMR analysis: interactions between Lys6-linked diUb and UBA domain of UBXN1

Adapted from:

Hameed, D.S., G.B.A. van Tilburg, R. Merkx, D. Flierman, H. Wienk, F. El Oualid, K. Hofmann, R. Boelens, and H. Ovaa, Diubiquitin-Based NMR Analysis: Interactions Between Lys6-Linked diUb and UBA Domain of UBXN1. *Front Chem*, 2019. 7: 921

Summary

Ubiquitination is a process in which a protein is modified by the covalent attachment of the C-terminal carboxylic acid of ubiquitin (Ub) to the ϵ -amine of lysine or N-terminal methionine residue of a substrate protein or another Ub molecule. Each of the seven internal lysine residues and the N-terminal methionine residue of Ub can be linked to the C-terminus of another Ub moiety to form 8 distinct Ub linkages and the resulting differences in linkage types elicit different Ub signalling pathways. Cellular responses are triggered when proteins containing ubiquitin-binding domains (UBDs) recognize and bind to specific polyUb linkage types. To get more insight into the differences between polyUb chains, all of the seven lysine-linked di-ubiquitin molecules (diUbs) were prepared and used as a model to study their structural conformations in solution using NMR spectroscopy. We report the synthesis of diUb molecules, fully ^{15}N -labeled on the distal (N-terminal) Ub moiety and revealed their structural orientation with respect to the proximal Ub. As expected, the diUb molecules exist in different conformations in solution, with multiple conformations known to exist for K6-, K48- and K63-linked diUb molecules. These multiple conformations allow structural flexibility in binding with UBDs thereby inducing unique responses. One of the well-known but poorly understood UBD-Ub interaction is the recognition of K6 polyubiquitin by the ubiquitin-associated (UBA) domain of UBXN1 in the BRCA-mediated DNA repair pathway. Using our synthetic ^{15}N -labeled diUbs, we establish here how a C-terminally extended UBA domain of UBXN1 confers specificity to K6 diUb while the non-extended version of the domain does not show any linkage preference. We show that the two distinct conformations of K6 diUb that exist in solution converge into a single conformation upon binding to this extended form of the UBA domain of the UBXN1 protein. It is likely that more of such extended UBA domains exist in nature and can contribute to linkage-specificity in Ub signalling. The isotopically labelled diUb compounds described here and the use of NMR to study their interactions with relevant partner molecules will help accelerate our understanding of Ub signalling pathways.

Introduction

Ubiquitin (Ub) is a small protein of 76 amino acids, involved in the post-translational modification of several proteins in cells [1, 2]. Ub is attached to a target protein in a process called ubiquitination which employs a specific combination of three enzyme classes: Ub activating enzyme E1, Conjugating enzyme E2 and Ub ligase E3 [3]. On the other hand, ubiquitin can be removed from its substrates by enzymes called deubiquitinases (DUBs) [4]. Ub is attached to a target protein as a monomer or as a polymeric chain (polyUb) in which individual Ub molecules are attached via their C-terminal residue to one of the seven lysine residues (K6, K11, K27, K29, K33, K48 and K63) or the N-terminal methionine residue of other Ub molecules [5, 6]. Different types of Ub modifications cause different responses, such as regulation of protein turnover and DNA-repair signalling and are therefore ubiquitination is essential in maintaining cellular homeostasis. The polyUb chains vary in length, type of linkage (homotypic or branched) and the position of the modified lysine residues in target proteins [7]. Recognition of different polyUb chains by Ub binding domains (UBDs) is essential for stimulation of Ub signalling pathways.

The enzymatic assembly of all but K27-linked homotypical ubiquitin chains can be achieved by using the required combination of ubiquitinating E1-E2-E3 enzymes. [8-11] However, there is lack of control over the length of polyUb chains generated when using enzymatic methods and this often requires either mutating the Ub monomer to halt the chain extension or using extensive purification methods to separate different Ub polymers. In addition, such techniques are known for being less selective and require post-synthesis clean-

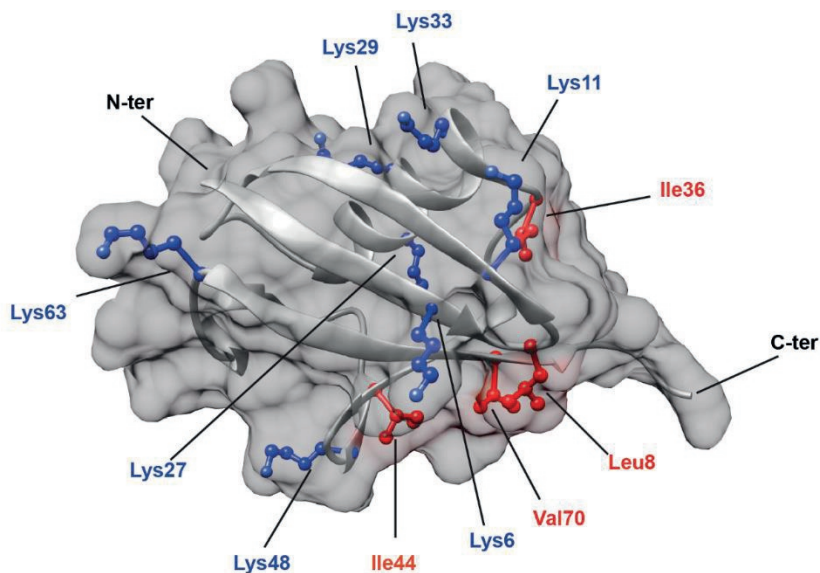


Figure 1: Structure of Ub (PDB: 1UBQ) showing the positions of all seven lysine residues (coloured in blue). In addition, hydrophobic residues (coloured in red) known to be involved in protein interactions are also highlighted.

up of undesired chains using chain-specific DUBs. This results in low yields and long preparation times. To circumvent this, in the past years, we and others have reported the synthesis of ubiquitin chains using chemical tools. [12-15] The use of a thiolysine handle at the sites of ubiquitination and the omission of enzymes resulted in the generation of diUbs of all seven isopeptide linkages [16]. These chains have been used extensively to study the biochemical properties of DUBs [17, 18].

To study the structural behaviour of diUb molecules in solution by nuclear magnetic resonance spectroscopy (NMR), segmental isotope-labelled diUb reagents can be a valuable tool. Such a diUb molecule consists of a labelled Ub moiety linked to an unlabeled Ub moiety at defined positions. Synthesis of labelled diUb molecules has been reported previously relying on expressing recombinant Ub using an evolved tRNA/tRNA-synthetase system, followed by selective deprotection, chemical ligation and purification of diUb molecules [19, 20]. These diUb molecules can be used to study the intermolecular interactions with other proteins involved in the ubiquitin pathway.

It has been reported that Ub chain interactions with other proteins frequently involve a hydrophobic patch containing residues such as Leucine 8, Isoleucines 36 and 44, and Valine 70 on the ubiquitin surface (Figure 1, labelled in red) [21]. This patch is also involved in interactions between the Ub monomers in a diUb molecule or in polyUb chains. However, the position of interacting residues and the strength of the interaction between monomers differ for each Ub linkage [22]. Although structural information on commercially available K48 [23-25] and K63 [26-29] Ub chains and other atypical Ub chains of K6- [10, 30], K11- [31-33], K27- [34], K29- [35] and K33- [9, 20, 36] linkages is available, a comparative study on diUb structural dynamics in solution is necessary to get an idea on the differences in structure of different Ub linkages. Since structure-function relationships are known to be directive in ubiquitin signalling, it is essential to uncover the structural details of diUb

molecules. For obtaining structural details, X-ray crystallography and increasingly also single-particle EM can be used to obtain high-resolution snapshots of protein folding and interactions of diUb molecules with some of their interacting proteins. On the other hand, NMR spectroscopy can provide a more dynamic view on structural transitions due to changes in environmental conditions and allows kinetic analyses of binding and dissociation between proteins and their interacting partners. In this study, we synthesized all seven isopeptide-linked diUbs using native chemical ligation of different proximal lysine-Ubs to a distal ^{15}N -labeled Ub. A comparative study on the interactions between the ^{15}N -labelled distal Ub and the unlabeled proximal Ub for each of the diUb linkages showed different interaction details in good agreement with previously reported data [37, 38]. Furthermore, we demonstrate here the usefulness of these tools for gaining structural insights into the selective recognition of a unique Ub-binding domain (UBD) for a diUb linkage.

Each ubiquitin linkage-type leads to a different response in cells, based on their recognition by specific proteins containing a UBD. UBDS provide a structural basis for different responses by recruiting Ub chains and other proteins associated in their respective pathway. For example, the DNA repair pathway is one of the crucial pathways in cells that utilize polyUb signalling and is essential in maintaining genomic integrity during or after cell division. DNA damage can be repaired by several mechanisms [39]. Among them, Non-Homologous End Joining (NHEJ) and Homologous Recombination (HR) are the most prevalent DNA-damage repair pathways. It has been observed that a Ubiquitin ligase called BRCA1 is involved in both of these DNA repair pathways. BRCA1 is an oncogene that is mainly associated with the prevalence of breast cancer [40].

The BRCA-mediated DNA repair pathway involves the recognition of K6 polyubiquitin chains on BRCA1 protein by another protein called UBXN1 [41]. The UBXN1 protein contains a UBD that belongs to the family of ubiquitin-associated domain (UBA) at its N-terminal tail [42]. The UBA domain is one of the earliest types of defined ubiquitin-binding domains described in literature [43]. These domains are short (about 45 amino acids) polypeptide sequences and are frequently observed in the enzymes associated with the ubiquitin machinery. The UBA domains usually consists of three alpha-helix modules which include a highly conserved hydrophobic surface that can bind efficiently with hydrophobic areas of Ub or polyUb chains [44]. The UBA sequences are conserved among proteins and enzymes involved in the proteasome degradation pathway [45] and in DNA repair [46].

Although it has been established that the UBA domain of UBXN1 can specifically recognize a K6 polyUb chain attached to the BRCA1 Ub ligase [42], the mode of interaction between the isolated UBA domain and the K6-Ub chain is largely unknown. Using our synthetic diUbs and biophysical techniques, we established how only an extended version of the UBA domain (UBAext1-52) of the UBXN1 protein binds selectively to K6 diUb. To illustrate the interaction of K6 diUb with UBAext1-52 of the UBXN1 protein, we monitored their titration by NMR and revealed which residues in the distal Ub of the K6 diUb molecule are important for this interaction. Understanding this interaction between the extended UBA domain and K6 Ub chains will help in understanding the interaction preference over other Ub chains.

Materials and methods

Expression of UBE1 enzyme and ^{15}N isotopic labelling of ubiquitin

All chemicals were obtained from Sigma unless stated otherwise. The ubiquitin-activating enzyme (UBA1) was recombinantly expressed with N-terminally fused hexahistidine tag (His6-tag). The enzyme was expressed in BL21 *E.coli* cells by adding 1 mM IPTG when the OD600 reached 0.6, followed by culturing the cells at 18°C overnight.

Cells were then sonicated in a lysis buffer containing 20 mM Tris-HCl, 250 mM NaCl and 5 mM 2-Mercaptoethanol at pH 8. The supernatant was incubated with TALON® metal affinity resin and after two washing steps, the UBA1 was eluted at 250 mM Imidazole concentration in the elution buffer. The imidazole was removed from the buffer using 10 kDa cut-off spin columns (Millipore). The final concentration of the enzyme was measured using a Nanodrop™.

¹⁵N-enriched ubiquitin was expressed as an untagged protein using a pET2A expression system in BL21 *E. coli* cells in minimal essential medium. The M9 minimal essential medium contained 50 mM Na₂HPO₄, 50 mM KH₂PO₄, 5 mM Na₂SO₄, 50 mM ¹⁵NH₄Cl, 2 mM MgSO₄, 0.01% glycerol, 0.001% glucose and 0.004% lactose (inducer). After expression by autoinduction at 37°C overnight, cells were spun down at 3700 G for 10 minutes and resuspended in Milli-Q™ water containing protease inhibitor cocktail tablets. Then the suspension was heated to 85°C for 30 minutes, cooled down to room temperature and added with 0.3 mg DNase per 50 mL suspension along with 10 mM MgSO₄. After heating again at 85°C for 30 minutes, the cell lysate was spun down at 20,000 rcf. The supernatant was purified by cation-exchange chromatography at 4°C using AKTA Unichromat 1500- “PRO” system (15 × 185 mm column packed with Workbeads™ 40 S) with two mobile phases: 50 mM NaOAc, pH 4.5 (solvent A), and 1 M NaCl in 50 mM NaOAc (solvent B), pH 4.5 (Flow-rate 5 mL/min). All fractions were checked on an SDS-PAGE gel. The pure fractions collected from the cation-exchange column were re-purified over a C18 Atlantis preparative reverse-phase HPLC on a Shimadzu Prominence system using two mobile phases: A = 0.05% TFA in water and B = 0.05% TFA in CH₃CN (Column temperature 40°C, flow rate 7.5 mL/min, UV-signal is measured at 230 and 254 nm). Typical ubiquitin yields were 80 mg/L of cell culture.

Preparation of lysine-linked diubiquitin molecules

The ¹⁵N-Ub-MESNa thioester was obtained according to a previously reported procedure with >95% yield, which was then purified using RP-HPLC and lyophilized [47]. ¹⁵N-Ub-MESNa thioester ligations were performed using the following conditions: 125 mM HEPES-NaOH pH 8; 100 mM MESNa; 10 mM MgCl₂; 10 mM ATP and 250 nM UBA1 enzyme at a concentration of 550 μM ¹⁵N Ubiquitin. The ¹⁵N-Ub-MESNa thioester was then purified using reversed-phase HPLC (RP-HPLC). Ub (K6, K11, K27, K29, K33, K48 and K63) δ-thiolysine derivatives were prepared using chemical synthesis on a solid phase. Diubiquitins were synthesized using a previously reported procedure [13]. Native chemical ligation was performed by adding equal amounts of ¹⁵N Ub MESNa thioester and thiolysine-Ub to a final concentration of 50 mg/mL in 6 M Gnd.HCl 0.2 M sodium phosphate buffer pH 8 containing 100 mM MPAA and 50 mM TCEP. After overnight ligation, the product was analyzed by LCMS and then diluted in desulphurization mix to a final concentration of 1 mg/ml protein (Diubiquitin). This mix contains 6 M Gnd.HCl 0.2 M sodium phosphate buffer pH 6.8, 200 mM TCEP, 50 mM reduced Glutathione, and 50 mM radical initiator VA-044 (2,2'-Azobis[2-(2-imidazolin-2-yl)propane]dihydrochloride). After overnight desulphurization, the product was analyzed by LCMS and purified with RP-HPLC.

Preparation of UBA peptides

UBA(1-42) and UBA(ext1-52) peptides were synthesized at 2 μmol scales, coupled with TAMRA on the N-terminus and purified by reversed-phase HPLC. Stock concentrations of TAMRA-UBA peptides were measured using a standard curve of TAMRA-K-G from 0-800 nM in 20 mM Tris pH 7.6 and 150 mM NaCl.

Diubiquitin-based NMR analysis

The amino acid sequence of the UBA domain of the UBXN1 protein is as follows:

10 20 30 40 50
MAELTALESL IEMGFPRGRA EKALALTGNQ GIEAAMDWLM EHEDDPDVDE PL

Analysis of ubiquitin and diubiquitin molecules

The Ub and diUb molecules were analyzed by 12 % Nu-PAGE SDS gel electrophoresis using MES buffer and Seablue plus 2® as a protein marker. Isolated products with an expected molecular weight (MW) of 17,212 Da were observed as a single band in the gel at around 17 kDa. The MW of the product were also confirmed by LC/MS using a Phenomenex Kinetex C18 (2.1 × 50 mm, 2.6 μm) column (flow rate: 0.8 mL/min; runtime: 6 min; mobile phases: A = 1% CH₃CN, 0.1% formic acid in water and B = 1% water and 0.1% formic acid in CH₃CN; column T = 40°C. Protocol: 0–0.5 min: 5% B; 0.5–4 min: 5–95% B gradient; 4–5.5 min: 95% B). Final yields were measured after freeze-drying the product.

For Circular Dichroism (CD) measurements, a JASCO CD J1000 machine was used (UMC, Utrecht, the Netherlands). Samples were dissolved in DMSO and then diluted in NMR buffer containing 20 mM NaH₂PO₄ pH 6.8 to a final concentration of 4 μM. Measurements were performed at 25°C using wavelengths ranging from 260 nm to 185 nm in a span of 100 mdeg. The scanning speed was 20 nm/min and measurements from 10 experiments were averaged. After CD measurements, the samples were subjected to BCA assay to determine actual concentrations. Based on the observed values of CD measurements and concentration from BCA assay, CD plots were prepared.

NMR measurements

Freeze-dried ubiquitin and diubiquitin samples were dissolved in 5% DMSO (Biosolve) in Milli-Q® water and then redissolved in NMR buffer containing 20 mM NaPO₄ pH 6.8 and 10 % D₂O. Then, samples were taken in 15 ml 3.5 kDa Millipore spin filter tubes and spun-washed with three volumes of NMR buffer until DMSO was almost completely removed (LC/MS analysis). Concentrated samples were diluted to 500 μL with NMR buffer and the final concentration was determined using BCA assay using ubiquitin as standard. The pH was carefully measured using a Mettler TOLEDO pH probe.

All NMR studies were carried out on a Bruker 900 MHz spectrometer with a TCI cryoprobe, at 298 K (25°C). [¹H, ¹⁵N] HSQC-spectra were acquired, processed and calibrated using standard methods. Chemical Shift Perturbations (CSPs) were calculated by comparing the [¹H, ¹⁵N] HSQC spectra of mono Ub with that of each of the diUb molecules/ The CSP was calculated according to the following formula

$$CSP = \sqrt{(0.2\Delta\delta N)^2 + (\Delta\delta H)^2}$$

where ΔδH and ΔδN are the chemical shift differences for ¹H and ¹⁵N respectively. The spectra of K6 diUb indicated two different co-existing conformations. An ‘open conformation’ was assigned based on similarity with the mono-Ub spectrum.

Fluorescence polarization and microscale thermophoresis measurements

Fluorescence polarization (FP) measurements were performed at room temperature preceded by overnight incubation of UBA(ext1-52) domain with diubiquitin at 4°C. Total assay volume was 20 μL in black 384-well plates (low volume, flat bottom, non-binding surface; Corning®; ref 3820). All diubiquitin variants and concentrations were measured in triplicate. The concentration of synthetic TMR-labeled UBA domain was unchanged at 5 nM while diubiquitin was added in six steps of increasing concentrations from 0.78 – 25 μM. A UBA domain-only control (0 μM diubiquitin) was used to normalize measured FP values to

0. For these measurements, native diubiquitins were used and prepared as described previously [13]. DiUbs were additionally purified by gel filtration on a HiLoad 16/600 superdex 75 pg column (GE Healthcare) in 20 mM Tris pH 7.6 and 150 mM NaCl. The measurements were carried out in a FP binding buffer (20 mM Tris pH 7.6, 150 mM NaCl, 0.5 mg/ml BGG, 1% TX-100). Before each measurement, the plates were briefly centrifuged for 1 min at 4°C and 500 G. Read-out was performed on a PHERAstar plate reader (BMG labtech) using a TAMRA filter. Statistical analyses were performed with GraphPad Prism 7 software using non-linear regression analysis (one site binding (hyperbola)).

Microscale thermophoresis (MST) measurements were carried out using the synthetic TAMRA-UBAdomains in FP binding buffer. Concentrations of K6 diUb ranged from 1.53 nM – 50 μM. Samples were incubated for 30 min to allow binding and measured in hydrophobic capillaries on a Monolith NT.115 reader (NanoTemper Technologies, Munich, Germany) using 30% LED and 40% IR-laser power. The analysis was performed with GraphPad Prism 7 software using non-linear regression analysis (log (inhibitor) vs. response (three parameters)).

Results

DiUb synthesis and validation by gel, LCMS

Diubiquitin molecules were synthesized using our previously established native chemical ligation procedure (Figure 2) [13]. Briefly, the different proximal Ub moieties, containing a δ-thiolslysine building block instead of a lysine residue, were generated using Fmoc SPPS.

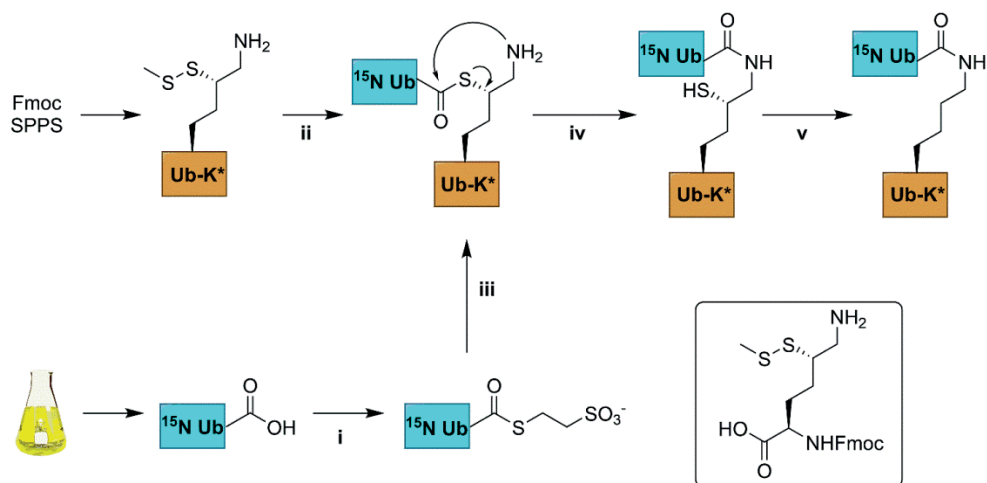


Figure 2: Schematic representation of the synthesis of ^{15}N -labelled diUb. ^{15}N -Ub was expressed in a bacterial expression system; thiolslysine (inset) containing Ub was synthesized from Fmoc-based SPPS. i) 100 nM Ube1, 100 mM MESNa, pH 8; ii) 50 mM TCEP, 6M Gnd.HCl; iii) Ub-thiolslysine after step ii, 100 mM MPAA, 6M Gnd.HCl, pH 8; iv) room temperature, overnight incubation; v) buffer exchange to remove MPAA, 100 mM TCEP, 100 mM VA-044, 6 M Gnd.HCl, pH 7.

The distal ^{15}N -Ub part was prepared by recombinant bacterial expression in ^{15}N -ammonia enriched M9 minimal medium and converted to ^{15}N -Ub MESNa thioester using Ube1 enzyme and MESNa. The proximal and ^{15}N -distal Ub precursors were ligated using native

Diubiquitin-based NMR analysis

chemical ligation conditions. The product was then subjected to chemical desulfurization using TCEP and VA-044 and finally purified by reversed-phase HPLC.

The purified product was dissolved in DMSO and refolded into NMR buffer (20 mM NaPO₄ pH 6.8 and 10 % D₂O). ¹⁵N-Ub was also purified by HPLC and refolded using the same procedure. To check for proper folding, the products were examined by Circular Dichroism (CD) using commercially available Ub as a control. Based on SDS-PAGE analysis (Figure S1A), the CD spectra (Figure S1B) and LC/MS analysis, the distal ¹⁵N labelled diUbs (Figures S14 to S21) are found to be pure and properly refolded.

Comparison of NMR data of monoUb and diUb molecules

By NMR, a 2D [¹H, ¹⁵N] HSQC spectrum was obtained for ¹⁵N-Ub (Figure S2). Although most of the signals were identified and assigned according to a previously reported data [48], signals corresponding to Met1, Glu24 and Gly53 backbone amides were missing. The data showed that monoUb is properly folded.

We compared the [¹H, ¹⁵N] HSQC spectra of each of the different ¹⁵N-diUb molecules (hereafter referred to as diUbs) to that of monomeric ¹⁵N-Ub to reveal interactions between the distal Ub and proximal Ub moieties. Chemical shift perturbations (CSP) were calculated from ¹H and ¹⁵N resonance frequency-differences between signals of the same residue in both monoUb and diUb spectra. This was plotted in a graph, illustrating the influence of the attached proximal Ub on residues in the ¹⁵N-distal Ub moiety (Figure 3). Previously using a similar approach, the K48 [23, 49, 50] and K63 [29, 51] diUbs have been extensively studied. In our experiments, we also analyzed the NMR spectrum of all other diUb molecules.

CSPs are useful in determining the changes in the local environment of amino acids, which can be attributed to direct or indirect interactions but cannot be differentiated as such. All diUb spectra showed a common CSP behaviour in the C-terminal region of the distal Ub module, where the isopeptide linkage with the proximal Ub module is located. However, the hydrophobic region in Ub including the residues of Leu8, Ile36, Ile44 and Val70 and its surroundings also showed CSPs to a varying degree of magnitude and signal shift directions. In the case of K6 diUb, spectral changes were mostly observed for Leu8, Ile36 and a small region in the second beta-sheet covering residues Thr12, Ile13 and Thr14. K11 diUb showed similar behaviour encompassing residues Thr9, Ile13, Thr14 and Arg42. Here, Lys48, which is in the hydrophobic region surrounding Ile44 residue, was also disturbed. The elusive K27 diUb showed changes for Thr9 and Lys48 nearby the hydrophobic patch that surrounds Leu8 and Ile44 residues respectively. K29 diUb showed disturbances in Leu8, Ile13, Thr14 and Lys48, similar to that of K11 diUb. Intriguingly, the spectra of K27 diUb and K29 diUb show variation likely because the lys29 residue in K29 diUb is more solvent-exposed compared to lys27 in K27 diUb. Similar effects as with K29 diUb were also observed for K33 diUb. K48 diUb, which is the most studied so far, showed CSPs for Val5, Ile13, areas around Ile44 and Val70, encompassing the hydrophobic patch of Ub, suggesting a compact folding as had been observed in X-ray crystal structures of K48 polyUb chains [52]. Finally, K63 diUb shows the least interactions between the distal Ub and proximal Ub, in line with the reported open conformations known for K63 linked Ub chains. Comparing the overall CSPs of each of the diUbs measured in our NMR experiment, we observed that K6 diUb, K11 diUb, K29 diUb and K48 diUb showed more perturbations than K27 diUb, K33 diUb and K63 diUb.

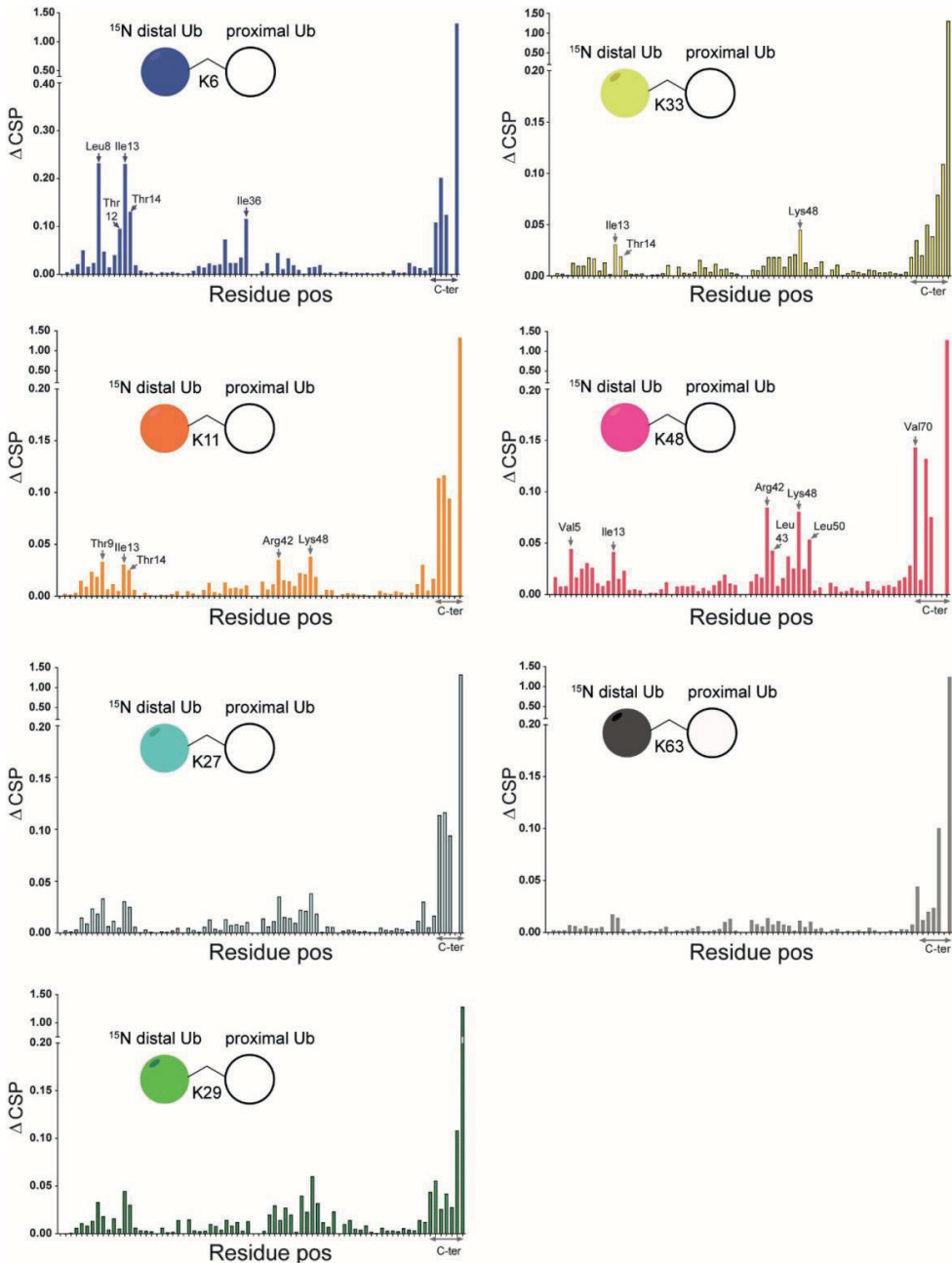


Figure 3: CSPs calculated for all isopeptide linked diUbs by comparison of ^{15}N - ^1H HSQC spectrum of mono-Ub with that of each of the ^{15}N -labelled diUb. Pictorial representations of each of the diUbs are shown (in each panel). In general, the C-terminal residues in all diUbs show CSP due to their covalent bonding with the second unlabeled Ub. However, other residues also show changes, indicating their possible interaction with the unlabeled proximal Ub. The residues that show major CSP besides the C-terminal region are labeled.

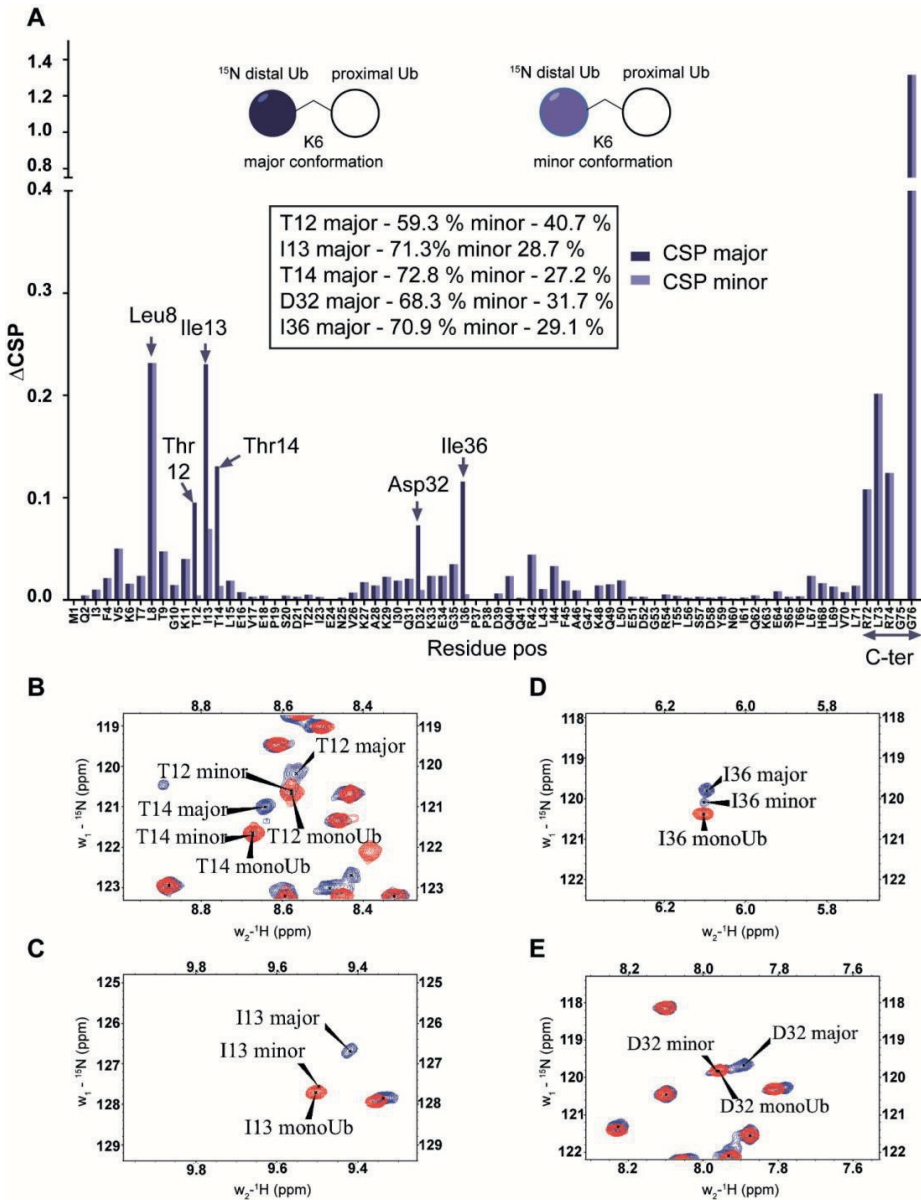


Figure 4: *A:* Chemical shift perturbations calculated by comparing the ^{15}N - ^1H spectrum of mono-Ub and the distally ^{15}N -labelled K6-diUb (structural representation in inset). Although most of the signals are less affected, certain residues like Leu8, Thr12-Thr14, Ile36 and the C-terminal tail from Arg72 to Gly76 are all shifted significantly. This indicates a change in the electronic environment of these residues, which may be attributed to interactions with the unlabeled proximal-Ub. Leu8 and Ile36 show a considerable migration relative to other residues. In addition, signal doubling is observed for Asp32 and Ile36 in K6-diUb. *B-E:* NMR spectral regions showing ^{15}N - ^1H peaks of Thr12, Ile13, Thr14, Asp32 and Ile36 of K6 diUb (blue) compared with monoUb (red).

Of particular interest was the K6 diUb spectrum which showed signal-doubling for Thr12, Ile13 and Thr14 and residues Asp32 and Ile36 (Figure 4A-E). After ruling out the presence of impurities in the K6 diUb sample (Figures S1A, S15), we further analyzed this phenomenon. Based on the reported crystal structure for K6 diUb, the region around Asp32 and Ile36 is away from the interface between the two Ub moieties [30]. Our data suggest that there is a second conformation in solution. Assuming that relaxation properties and NMR lineshapes between the two conformations are similar we estimate the major and minor populations in an approximate ratio of 70:30 for K6 diUb (Figure 4). In the major conformation, Leu8, Asp32 and Ile36 could interact with Thr12, Ile13 and Thr14 residues ('loop-in' conformation) which is in agreement with a compact diUb fold. In the minor conformation, there is less effect from Ile36 and therefore less perturbations are seen in Thr12, Ile13 and Thr14 residues ('loop-out' conformation) indicating that this K6 diUb conformation is less compact than the closed one but comparable to K48 diUb.

A novel C-terminally extended UBA domain of the UBXM1 protein binds specifically to K6-linked diubiquitin *in vitro*

K6-linked polyubiquitin chains are known to be involved in BRCA-mediated DNA repair [41]. The BRCA1 protein forms a complex with BARD1 to gain its ubiquitin ligating activity. In addition to ubiquitinating many substrates involved in the DNA repair pathway with K6-linked polyUb chains [53], the BRCA1-BARD1 heterodimer complex can also auto-ubiquitinate itself with K6-linked polyUb chains [42, 54]. In this auto-ubiquitinated state, BRCA1-BARD1 ligase activity is significantly reduced by binding to the protein UBXM1 [42]. UBXM1 contains an N-terminal UBA domain (residues 1-42) that binds to K6-linked polyubiquitin chains conjugated to BRCA1, while the C-terminal sequences of UBXM1 bind the BRCA1/BARD1 heterodimer in a ubiquitin-independent fashion (Wu-Baer et al., 2010). However, the isolated UBA(1-42) domain of UBXM1 did not bind with K6 polyUb chains, while deletion of this section in full length protein did abolish K6 interaction. This implied to us that there might be more residues beyond the UBA domain that are important for the K6-linked ubiquitin interaction [42].

		normal UBA																																																					
UBXM1		A	E	L	T	A	L	E	S	L	I	E	M	G	F	P	R	G	R	A	E	K	A	L	A	T	G	N	Q	G	I	E	A	A	M	D	W	L	M	E	H	E	D	P	D	V	D	E	P	L	E	T	P		
UBASH3A		S	S	P	S	L	L	E	P	L	I	A	M	G	F	P	V	H	T	A	L	K	A	L	A	A	T	G	R	K	T	A	E	E	A	L	A	W	L	H	D	H	C	N	D	P	S	L	D	D	P	I	P	Q	E
UBASH3B		K	H	G	S	A	L	D	V	L	L	S	M	G	F	P	R	A	R	A	Q	K	A	L	A	S	T	G	G	R	S	V	Q	A	A	C	D	W	L	F	S	H	V	G	D	P	F	L	D	D	P	L	P	R	E
UBAC1		V	D	E	A	A	L	R	Q	L	T	E	M	G	F	P	E	N	R	A	T	K	A	L	Q	L	N	.	M	S	V	P	Q	A	M	E	W	L	I	E	H	A	E	D	P	T	I	D	T	P	L	P	G	Q	
USP5	1	L	D	E	S	V	I	Q	L	V	E	M	G	F	P	M	D	A	C	R	K	A	V	Y	T	G	N	S	G	A	E	A	A	M	N	W	V	M	S	H	M	D	D	P	D	F	A	N	P	L	I	L	P		
USP5	2	P	P	E	D	C	V	T	T	I	V	S	M	G	F	S	R	D	Q	A	L	K	A	L	R	A	T	N	.	S	L	E	R	A	V	D	W	I	F	S	H	I	D	D	L	D	A	E	A	A	M	D	I	S	
USP13	1	I	D	E	S	S	V	M	Q	L	A	E	M	G	F	P	L	E	A	C	R	K	A	V	Y	T	G	N	M	G	A	E	V	A	F	N	W	I	T	V	H	M	E	E	P	D	F	A	E	P	L	T	M	P	
USP13	2	P	P	E	E	I	V	A	I	T	S	M	G	F	O	R	N	Q	A	I	Q	A	L	R	A	T	N	.	N	L	E	R	A	L	D	W	I	F	S	H	P	E	F	E	E	D	S	D	F	V	I	E	M		

Table 1: Comparison of UBA domain sequences from different Ub binding proteins. The C-terminal extension adds about 10 amino acids at the C-terminal end of the conventional UBA domain. Moreover, all extended UBA domains have a totally invariant WxxxH motif within the 3rd helix. While this region is part of the conventional UBA fold, the conservation of this motif is only found in extended UBA-domain-containing members.

To study this in more detail, we set out to investigate the specificity of the UBXM1 UBA domain for K6 diUb molecules using a Fluorescence Polarization (FP) binding assay in which TAMRA-labeled UBA peptide was added to different concentrations of unlabeled diUbs of

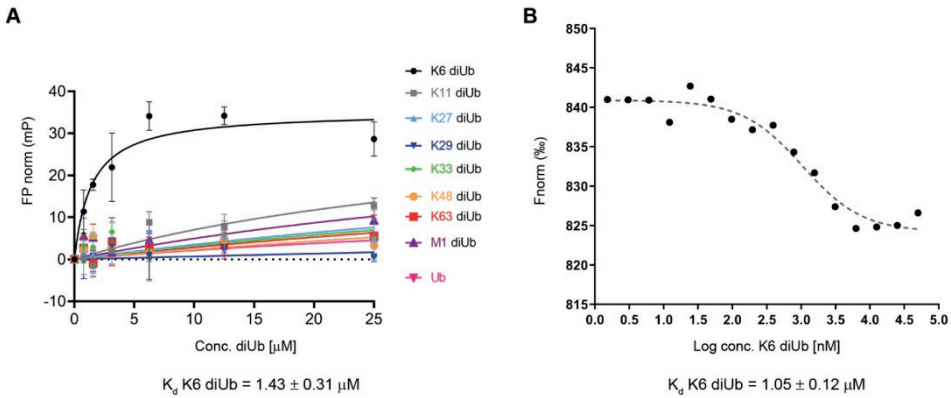


Figure 5: *A:* Fluorescence polarization assay using a TAMRA-labeled UBAXN1 UBA(ext1-52) domain and different concentrations of all 8 homotypical diUbs and monoUb. *B:* Microscale thermophoresis binding curve of K6 diUb to TAMRA-labeled UBAext1-52 from UBAXN1. These experiments show the preference and tight binding of UBA(ext1-52) to K6 diUb.

all linkage types. Consistent with the findings of Wu-Baer *et al*, we also did not observe binding of K6 diubiquitin with the canonical UBA domain (1-42) of UBAXN1 (Figure S10) [42]. On comparing the UBA domains of other proteins, we found that the 10 amino acids following the C-terminus of all conventional UBA domains that we compared showed the existence of a conserved sequence (Table 1). Interestingly when looking at the alignment, a previously unnoticed WxxxH motif was found to be conserved only in the extended versions of the UBA domain and not the shorter ones. To investigate whether this C-terminally extended version of the UBA domain of UBAXN1 had any effect on binding to K6 diUb, we repeated the FP binding assay with the UBA (1-52) domain. We observed a tight and linkage specific binding to K6 diubiquitin (Figure 5A). We quantified the linkage specific binding of UBA(ext1-52) to K6 diUb with an approximate K_d of $1.43 \pm 0.31 \mu\text{M}$ which was validated with an orthogonal technique called microscale thermophoresis (MST) (Figure 5B) and found a similar K_d value of $1.05 \pm 0.12 \mu\text{M}$.

Carefully analyzing the NMR structures of the isolated UBA domains of UBASH3A (pdb: 2CRN), UBASH3B (pdb: 2CPW), UBAC1 (pdb: 2DAI), USP5 UBA2 (pdb: 2DAK) and USP13 (pdb: 2LBC), we found that all three alpha-helices in the conventional UBA domain are structurally conserved whereas the first few residues of the 10 residues extending from the C-terminus starts from the last alpha-helix and then becomes largely unstructured (Figure 6). The C-terminal UBA extension in UBAXN1 seemingly adds to K6 diubiquitin specificity and further research is needed to investigate whether this holds true for the other proteins containing this conserved C-terminal UBA extension and thereby establishing a functional role of this conserved motif.

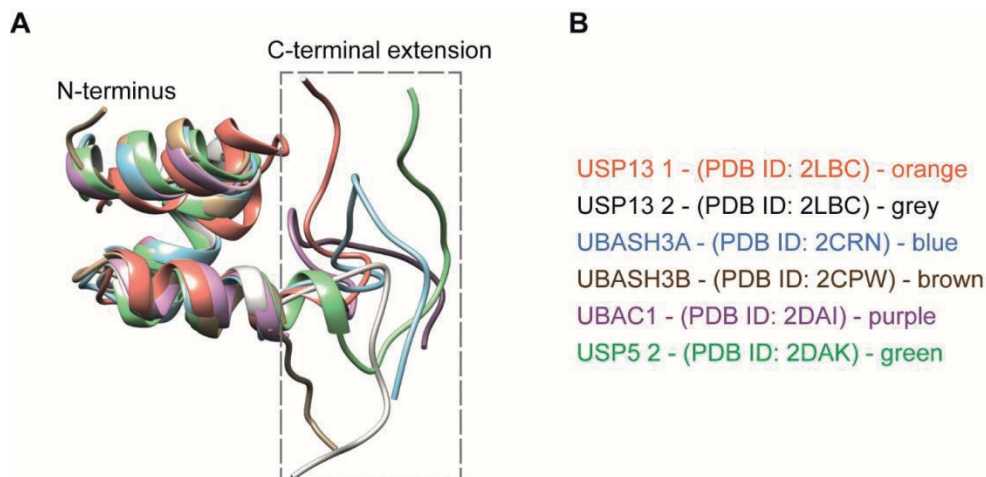


Figure 6: *A:* Structural comparisons of extended UBA domains. The C-terminal extension of all the UBA domains mentioned here is found to be disordered. *B:* The UBA-domain containing proteins are colour coded along with their respective PDB IDs.

NMR of K6 diUb with the UBA (1-52) domain of UBXN1 provides an insight into the mode of interaction

To further study the interaction between the UBA(ext1-52) domain of UBXN1 and K6 diUb, we titrated the UBA(ext1-52) with ^{15}N -K6 diUb and monitored this by NMR. Signals corresponding to Lys 48, Gln49, Leu69, Leu71 and Leu73 disappeared after adding more than 1 equivalent of UBA(ext1-52), suggesting that these sites are in direct interaction with the UBA peptide. For other residues, signal shifts were observed. The CSP results indicated a distinct role of the hydrophobic patch on the distal Ub moiety that encompasses the residues Leu8, Ile44, Ala46 and Val70. Moreover, the residues Val5 to Thr9, Lys11, Ile13 and Thr14, surrounding Leu8 of the distal Ub, were also perturbed (Figure 7A, S11). Interestingly, shifts in Thr12, Ile13 and Thr14 were observed and explained previously as the “loop-in” and “loop-out” conformations for K6 diUb [10].

Some signals that were split in the reference spectrum converged upon the addition of UBA(ext1-52) peptide. For example, Thr12, Ile13 and Thr14 were split in the unbound K6 diUb spectrum, but upon adding increasing concentrations of the UBA(ext1-52) peptide, their signals converged (Figure S12). This indicates that the two different conformations of K6 diUb change into a single conformation upon binding with UBA(ext1-52) peptide. The fact that Ile44 and Leu8 show higher CSP values implying that the K6 diUb molecule is changing preferring the ‘loop-out’ conformation upon interacting with the UBA peptide. However, residues Asp32 and Ile36 (Figure S13) remained doubled, suggesting that the binding to the UBA(ext1-52) domain has local effects, but does not affect the structure of the entire distal Ub module.

Diubiquitin-based NMR analysis

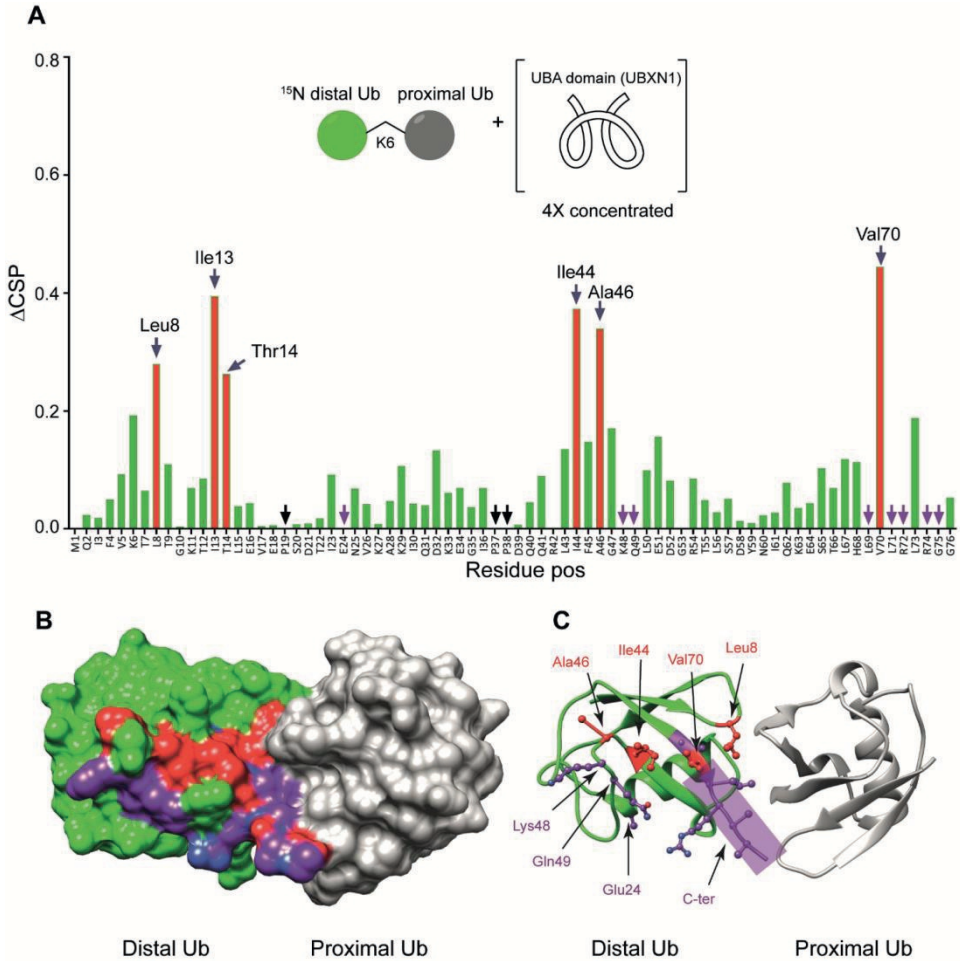


Figure 7: *A:* Unlabeled UBAext1-52 domain of UBXN1 was added in different concentrations to ¹⁵N-K6 diUb and the CSPs were monitored. At a ratio of 4:1 (UBA(ext1-52) domain:K6 diUb), residues Leu8, Ile44, Ala46 and Val70 (red bars, labelled) shifted more than the rest. Other residues like Tyr 59 remain unchanged. *B:* X-ray crystal structure of a K6 diUb (PDB: 2XEW) showing the residues that were perturbed according to CSP. Residues that shifted more are coloured in red. Residues whose signal disappeared upon addition of UBA(ext1-52) peptide are represented in purple. *C:* The same structure in figure B but showing the positions of side chains of the residues that were affected upon UBA(ext1-52) binding. Several perturbed residues are found to be positioned on the surface away from proximal Ub.

Using the known X-ray crystal structure of K6 diUb, the interacting residues were mapped on the Ub surface (Figure 7B and 7C). It appears that the residues interacting with the extended UBA peptide are positioned away from the proximal Ub moiety. The fact that the Leu8 residue of distal Ub is positioned at the interface between the distal Ub and proximal Ub moieties may suggest a dual role for this residue in interacting with both the proximal Ub and UBA peptide.

Discussion

Structures of all seven isopeptide-linked diUb molecules have been characterized using X-ray crystallography [26, 30, 33, 35, 36, 49, 55]. These crystal structures broadly fall into two categories: compact (K6, K48, K11, K27, K29, K33) and open (M1, K63) conformations [22]. Some Ub chains, however, are known to exist in intermediate forms in solution. For example, K48 chains obtain two different conformations in addition to several intermediate structures [50]. This structural flexibility is essential to facilitate polyUb signalling where K48 polyUb chains contribute to proteasomal degradation [51]. Although they mainly exist in a compact conformation, 10% of K48 Ub chains exist in an open conformation exposing the hydrophobic patches to make these accessible for interactions with proteins such as the UBA domain of hHR23A which leads to the recruitment of K48 poly-ubiquitinated substrates for proteasomal degradation [52]. In another study, the K48 diUb molecule has been found to exist predominantly in an open conformation [49]. It is clear that the existence of multiple conformations of K48 polyUb chains in cells are essential to bind with different proteins and elicit different responses and further research is needed to study the structural dynamics of K48 polyUb chains in cells. Although X-ray data can reveal different conformations of diUb molecules, solution NMR is convenient to study the dynamics between different conformations and interactions with specific binding domains. Moreover, control of the environment in NMR experiments offers freedom to study solution structures at different physiological conditions, pH or temperature. Given the advances in chemical synthesis of Ub and Ub molecules containing thiolysine, we were able to generate distally labelled diUbs and studied the interactions between the two Ub moieties from the perspective of distal Ub. The synthesis of Ub chains by genetic incorporation of protected lysine residues using modified tRNA synthetases followed by selective chemical ligation and deprotection has also enabled generating diUb molecules of all linkages which were then analysed by NMR spectroscopy [37]. Both approaches have demonstrated the advantages of using chemoenzymatic procedures to make diUb molecules to study their structural dynamics related to functionality.

For a better understanding of ubiquitin signalling pathway, it is essential to know how polyUb-specific interacting proteins recognize different polyUb chains. These interacting proteins often contain a specific UBD that can bind to specific polyUb chains, leading to different cellular responses. The best-studied Ub-interaction system is the K48 polyUb chain type and its corresponding interacting protein hHR23a in the proteasomal degradation system. Recently, it has been shown that hHR23a protein also recognizes K27 Ub chains, thereby implicating it in the DNA repair mechanism [37]. Although K48 chains are readily available for in-vitro studies, K27 chains are impossible to make via biochemical strategies and recombinant enzymes. Hence the chemical synthesis of these chains, such as shown in this study, may develop into a valuable tool in identifying the interacting proteins and establish a mechanism of binding.

DNA repair pathways are essential for the maintenance of the integrity of genomic DNA. The DNA repair pathway requires the efficient action of different protein complexes including the BRCA complex. Ubiquitination also plays an essential role in this pathway by adding different ubiquitin chains onto the proteins involved. For instance, the BRCA/ABRAXIS protein complex can be polyubiquitinated with K6, K48 and K63 polyUb chains by different sets of ubiquitin ligation enzymes and each of these modifications leads to different responses in the cell. Of special interest is the polyubiquitination with K6 chains which leads to recruitment of the DNA polymerase complex to restart DNA synthesis after DNA repair has been accomplished [56]. For K6 polyUb chains, UBXN1 acts as a specific

receptor protein and its UBA domain has been reported to be involved in chain recognition. However, the exact mode of binding has not been shown using any biophysical methods so far. In this study, we showed that to achieve binding to K6-linked ubiquitin, instead of the canonical UBXXN1 UBA (1-42) domain, an extended version of the UBXXN1 UBA domain, UBA(ext1-52), is needed. For the first time, we gain structural insight into the recognition of this elusive K6-specific ubiquitin-binding domain. Our results suggest that different conformations of K6 chains are locked into one dominant conformation upon binding with the UBXXN1 UBA(ext1-52) domain. The additional 10 amino acids long C-terminal extension of the conventional UBA domain is found to be conserved among different proteins and is therefore important to study this in more detail in future experiments.

Conclusion

We have synthesized all isopeptide-linked distally ^{15}N labelled diUb chains using native chemical ligation. This allowed us to study their conformations in solution and the interactions of the distal Ub moiety with the proximal Ub moiety by NMR. We also established that the additional C-terminal residues of the conventional UBA domain of UBXXN1 protein are essential in binding specifically with K6 diUb molecule. Upon comparing different diubiquitins of each linkage, we observed that K48-, K6-, K29- and K11- diUbs were in a relatively closed conformation while K33-, K27- and K63- diUbs were in a more open conformation. The CSPs revealed that K6 diUb exhibits the most closed conformation among all diubiquitins, whereas K63 exhibits the most open conformation. In general, calculating the total CSPs of all residues in each of the diUb spectra, excluding the C-terminal tail encompassing residues 70 to 76, provided a tentative overview on the degree

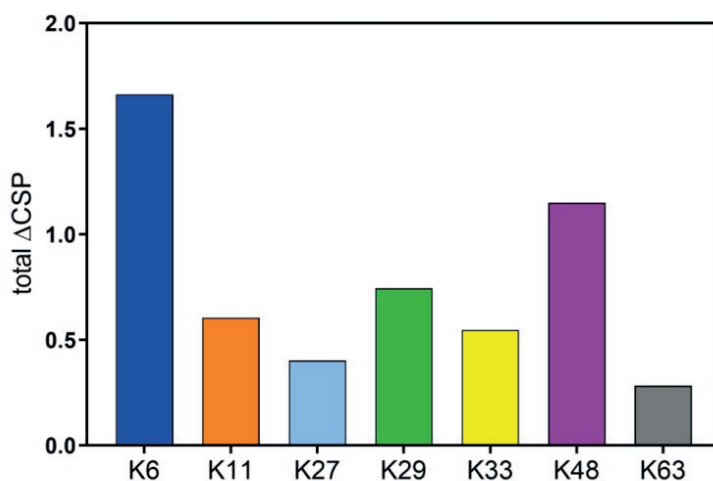


Figure 8: Sum of CSPs of residues in distal Ub of all diUbs excluding the C-terminal tail interactions which happen due to the proximity of isopeptide bond, and not exclusively due to the interaction between the interface of the distal and proximal Ub.

of compactness for each of the diUb molecules (Figure 8). In addition, we found that certain diUbs like K6 diUb, K48 diUb and K63 diUb exist in more than one conformation. For instance, in K6 diUb the residues Val5, Thr12, Ile13, Thr14, Asp32 and Ile36 gave rise to two signals.

Using our synthetic ^{15}N diUbs, we established how only an extended version of the UBA domain (UBAext1-52) of the UBXN1 protein binds selectively to K6 diUb, using NMR titration experiments, revealing the crucial residues in the distal Ub of K6 diUb important for this interaction. With this, we demonstrate the applicability of these ^{15}N labeled diUb chains as tools for gaining structural insights into the selective recognition of a unique UBD for a diUb linkage.

Conflict of Interest

FE and HO declare competing financial interests as shareholder of UbiQ Bio BV.

Author Contributions

D.S.H and R.M. prepared the Ub and diUb reagents for NMR measurements. G.v.T did the FP and MST measurements for UBA(ext1-52) and diUb interactions. H.W. measured the NMR spectra. D.S.H. and H.W. analyzed the NMR data. D.F., F.E.O and K.H. provided valuable suggestions and ideas. R.B. and H.O. supported the work with grants from NWO.

Funding

Work in the Ovaa lab was supported by NWO (VICI grant 724.013.002). NMR experiments were performed at the SONNMRLSF facility, financially supported by an NWO-Groot Grant 175.107.301.10.

Acknowledgements

We would like to thank Henk Hilkmann and Dris el Atmioui for providing synthetic ubiquitin mutants and ubiquitin-binding domains. We would like to thank Dr. Monique Mulder, Dr. Gerbrand J. van der Heden van Noort and Stephan Scherpe for critical reading.

Reference

1. Hochstrasser, M., *Ubiquitin-dependent protein degradation*. Annu Rev Genet, 1996. **30**: p. 405-39.
2. Hershko, A. and A. Ciechanover, *The ubiquitin system*. Annu Rev Biochem, 1998. **67**: p. 425-79.
3. Scheffner, M., U. Nuber, and J.M. Huibregtse, *Protein ubiquitination involving an E1-E2-E3 enzyme ubiquitin thioester cascade*. Nature, 1995. **373**(6509): p. 81-3.
4. Komander, D., M.J. Clague, and S. Urbe, *Breaking the chains: structure and function of the deubiquitinases*. Nat Rev Mol Cell Biol, 2009. **10**(8): p. 550-63.
5. Akutsu, M., I. Dikic, and A. Bremm, *Ubiquitin chain diversity at a glance*. Journal of Cell Science, 2016. **129**(5): p. 875-880.
6. Meierhofer, D., et al., *Quantitative analysis of global ubiquitination in HeLa cells by mass spectrometry*. J Proteome Res, 2008. **7**(10): p. 4566-76.
7. Li, W. and Y. Ye, *Polyubiquitin chains: functions, structures, and mechanisms*. Cell Mol Life Sci, 2008. **65**(15): p. 2397-406.
8. Zhang, M., et al., *Chaperoned ubiquitylation--crystal structures of the CHIP U box E3 ubiquitin ligase and a CHIP-Ubc13-Uev1a complex*. Mol Cell, 2005. **20**(4): p. 525-38.
9. Michel, M.A., et al., *Assembly and specific recognition of k29- and k33-linked polyubiquitin*. Mol Cell, 2015. **58**(1): p. 95-109.
10. Hospenthal, M.K., S.M. Freund, and D. Komander, *Assembly, analysis and architecture of atypical ubiquitin chains*. Nat Struct Mol Biol, 2013. **20**(5): p. 555-65.
11. Faggiano, S., C. Alfano, and A. Pastore, *The missing links to link ubiquitin: Methods for the enzymatic production of polyubiquitin chains*. Anal Biochem, 2016. **492**: p. 82-90.
12. Kumar, K.S., et al., *Total chemical synthesis of di-ubiquitin chains*. Angew Chem Int Ed Engl, 2010. **49**(48): p. 9126-31.
13. El Oualid, F., et al., *Chemical synthesis of ubiquitin, ubiquitin-based probes, and diubiquitin*. Angew Chem Int Ed Engl, 2010. **49**(52): p. 10149-53.
14. van der Heden van Noort, G.J., et al., *Synthesis of Poly-Ubiquitin Chains Using a Bifunctional Ubiquitin Monomer*. Org Lett, 2017. **19**(24): p. 6490-6493.
15. Moyal, T., et al., *Polymerization behavior of a bifunctional ubiquitin monomer as a function of the nucleophile site and folding conditions*. J Am Chem Soc, 2012. **134**(38): p. 16085-92.
16. Merkx, R., et al., *Scalable synthesis of γ -thiolysine starting from lysine and a side by side comparison with δ -thiolysine in non-enzymatic ubiquitination*. Chemical Science, 2013. **4**(12): p. 4494-4498.
17. Licchesi, J.D., et al., *An ankyrin-repeat ubiquitin-binding domain determines TRABID's specificity for atypical ubiquitin chains*. Nat Struct Mol Biol, 2011. **19**(1): p. 62-71.
18. Faesen, A.C., et al., *The differential modulation of USP activity by internal regulatory domains, interactors and eight ubiquitin chain types*. Chem Biol, 2011. **18**(12): p. 1550-61.
19. Castaneda, C., et al., *Nonenzymatic assembly of natural polyubiquitin chains of any linkage composition and isotopic labeling scheme*. J Am Chem Soc, 2011. **133**(44): p. 17855-68.
20. Castaneda, C.A., et al., *Segmental isotopic labeling of ubiquitin chains to unravel monomer-specific molecular behavior*. Angew Chem Int Ed Engl, 2011. **50**(47): p. 11210-4.

21. Sloper-Mould, K.E., et al., *Distinct functional surface regions on ubiquitin*. J Biol Chem, 2001. **276**(32): p. 30483-9.
22. Wang, Y., et al., *PolyUbiquitin chain linkage topology selects the functions from the underlying binding landscape*. PLoS Comput Biol, 2014. **10**(7): p. e1003691.
23. van Dijk, A.D., D. Fushman, and A.M. Bonvin, *Various strategies of using residual dipolar couplings in NMR-driven protein docking: application to Lys48-linked di-ubiquitin and validation against 15N-relaxation data*. Proteins, 2005. **60**(3): p. 367-81.
24. Ryabov, Y. and D. Fushman, *Structural assembly of multidomain proteins and protein complexes guided by the overall rotational diffusion tensor*. J Am Chem Soc, 2007. **129**(25): p. 7894-902.
25. Zhang, N., et al., *Structure of the s5a:k48-linked diubiquitin complex and its interactions with rpn13*. Mol Cell, 2009. **35**(3): p. 280-90.
26. Weeks, S.D., et al., *Crystal structures of Lys-63-linked tri- and di-ubiquitin reveal a highly extended chain architecture*. Proteins, 2009. **77**(4): p. 753-9.
27. He, F., et al., *Myosin VI Contains a Compact Structural Motif that Binds to Ubiquitin Chains*. Cell Rep, 2016. **14**(11): p. 2683-94.
28. Komander, D., et al., *Molecular discrimination of structurally equivalent Lys 63-linked and linear polyubiquitin chains*. EMBO Rep, 2009. **10**(5): p. 466-73.
29. Liu, Z., et al., *Lys63-linked ubiquitin chain adopts multiple conformational states for specific target recognition*. Elife, 2015. **4**.
30. Virdee, S., et al., *Engineered diubiquitin synthesis reveals Lys29-isopeptide specificity of an OTU deubiquitinase*. Nat Chem Biol, 2010. **6**(10): p. 750-7.
31. Matsumoto, M.L., et al., *K11-linked polyubiquitination in cell cycle control revealed by a K11 linkage-specific antibody*. Mol Cell, 2010. **39**(3): p. 477-84.
32. Castaneda, C.A., et al., *Unique structural, dynamical, and functional properties of k11-linked polyubiquitin chains*. Structure, 2013. **21**(7): p. 1168-81.
33. Bremm, A., S.M. Freund, and D. Komander, *Lys11-linked ubiquitin chains adopt compact conformations and are preferentially hydrolyzed by the deubiquitinase Cezanne*. Nat Struct Mol Biol, 2010. **17**(8): p. 939-47.
34. Gao, S., et al., *Monomer/Oligomer Quasi-Racemic Protein Crystallography*. J Am Chem Soc, 2016. **138**(43): p. 14497-14502.
35. Kristariyanto, Y.A., et al., *K29-selective ubiquitin binding domain reveals structural basis of specificity and heterotypic nature of k29 polyubiquitin*. Mol Cell, 2015. **58**(1): p. 83-94.
36. Kristariyanto, Y.A., et al., *Assembly and structure of Lys33-linked polyubiquitin reveals distinct conformations*. Biochem J, 2015. **467**(2): p. 345-52.
37. Castaneda, C.A., et al., *Linkage via K27 Bestows Ubiquitin Chains with Unique Properties among Polyubiquitins*. Structure, 2016. **24**(3): p. 423-36.
38. Castaneda, C.A., et al., *Linkage-specific conformational ensembles of non-canonical polyubiquitin chains*. Phys Chem Chem Phys, 2016. **18**(8): p. 5771-88.
39. Schwertman, P., S. Bekker-Jensen, and N. Mailand, *Regulation of DNA double-strand break repair by ubiquitin and ubiquitin-like modifiers*. Nat Rev Mol Cell Biol, 2016. **17**(6): p. 379-94.
40. Rosen, E.M., et al., *BRCA1 gene in breast cancer*. J Cell Physiol, 2003. **196**(1): p. 19-41.
41. Ohta, T., K. Sato, and W. Wu, *The BRCA1 ubiquitin ligase and homologous recombination repair*. FEBS Lett, 2011. **585**(18): p. 2836-44.

Diubiquitin-based NMR analysis

42. Wu-Baer, F., T. Ludwig, and R. Baer, *The UBXN1 protein associates with autoubiquitinated forms of the BRCA1 tumor suppressor and inhibits its enzymatic function*. Mol Cell Biol, 2010. **30**(11): p. 2787-98.
43. Hofmann, K. and P. Bucher, *The UBA domain: a sequence motif present in multiple enzyme classes of the ubiquitination pathway*. Trends Biochem Sci, 1996. **21**(5): p. 172-3.
44. Mueller, T.D. and J. Feigon, *Solution structures of UBA domains reveal a conserved hydrophobic surface for protein-protein interactions*. J Mol Biol, 2002. **319**(5): p. 1243-55.
45. Chen, L., et al., *Ubiquitin-associated (UBA) domains in Rad23 bind ubiquitin and promote inhibition of multi-ubiquitin chain assembly*. EMBO Rep, 2001. **2**(10): p. 933-8.
46. Kozlov, G., et al., *Structural basis of ubiquitin recognition by the ubiquitin-associated (UBA) domain of the ubiquitin ligase EDD*. J Biol Chem, 2007. **282**(49): p. 35787-95.
47. Oualid, F.E., et al., *Synthesis of atypical diubiquitin chains*. Methods Mol Biol, 2012. **832**: p. 597-609.
48. Cornilescu, G., et al., *Validation of protein structure from anisotropic carbonyl chemical shifts in a dilute liquid crystalline phase*. Journal of the American Chemical Society, 1998. **120**(27): p. 6836-6837.
49. Hirano, T., et al., *Conformational dynamics of wild-type Lys-48-linked diubiquitin in solution*. J Biol Chem, 2011. **286**(43): p. 37496-502.
50. Lai, M.Y., et al., *Structural and biochemical studies of the open state of Lys48-linked diubiquitin*. Biochim Biophys Acta, 2012. **1823**(11): p. 2046-56.
51. Jacobson, A.D., et al., *The lysine 48 and lysine 63 ubiquitin conjugates are processed differently by the 26 S proteasome*. J Biol Chem, 2009. **284**(51): p. 35485-94.
52. Varadan, R., et al., *Structural determinants for selective recognition of a Lys48-linked polyubiquitin chain by a UBA domain*. Mol Cell, 2005. **18**(6): p. 687-98.
53. Sato, K., E. Rajendra, and T. Ohta, *The UPS: a promising target for breast cancer treatment*. BMC Biochem, 2008. **9 Suppl 1**: p. S2.
54. Chen, A., et al., *Autoubiquitination of the BRCA1*BARD1 RING ubiquitin ligase*. J Biol Chem, 2002. **277**(24): p. 22085-92.
55. Pan, M., et al., *Quasi-Racemic X-ray Structures of K27-Linked Ubiquitin Chains Prepared by Total Chemical Synthesis*. J Am Chem Soc, 2016. **138**(23): p. 7429-35.
56. Morris, J.R. and E. Solomon, *BRCA1 : BARD1 induces the formation of conjugated ubiquitin structures, dependent on K6 of ubiquitin, in cells during DNA replication and repair*. Hum Mol Genet, 2004. **13**(8): p. 807-17.

Supplementary information

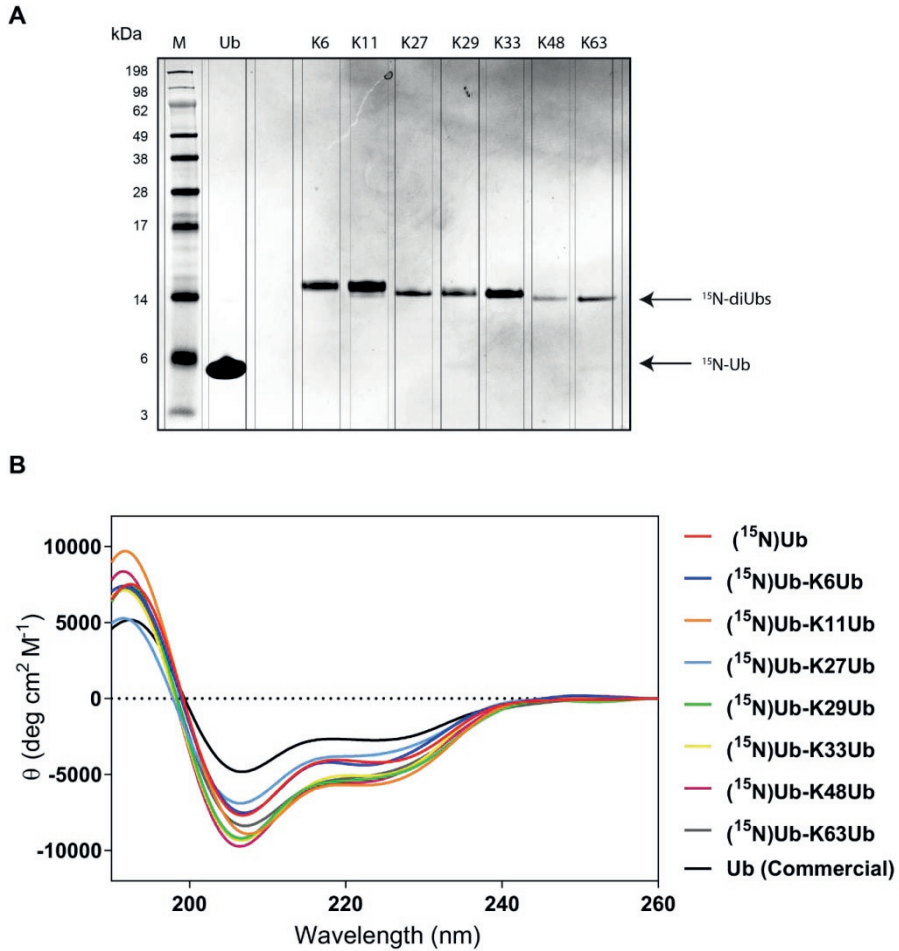


Figure S1: *A: SDS-PAGE analysis of purified NMR samples. ^{15}N -Ub was compared with ^{15}N -diUbs which shows almost no contamination with monoUb samples. **B:** Circular Dichroism spectrum of ^{15}N -Ub and ^{15}N -diUbs compared with expressed Ub from a commercial source (Boston Biochem CAT: U-100H).*

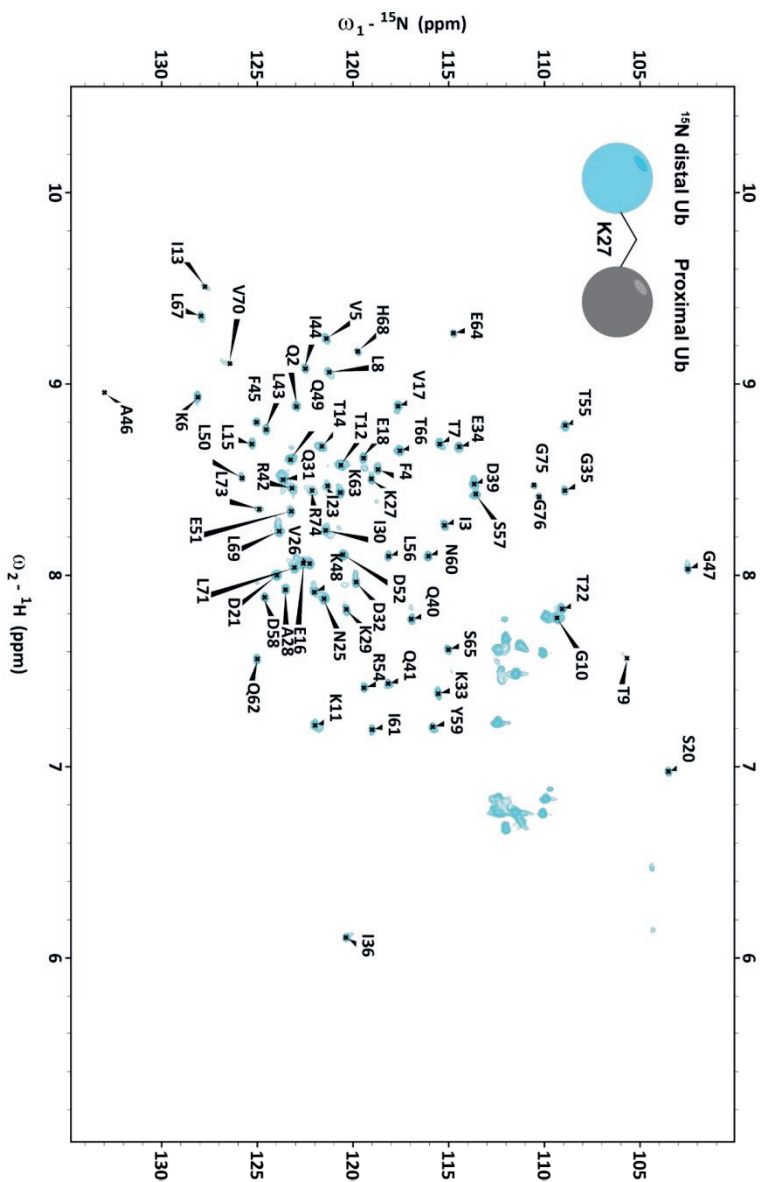


Figure S5: NMR spectrum of ^{15}N -Ub-K27-Ub (K27 diUb). The NMR (^1H - ^{15}N HSQC) spectrum of ^{15}N -labelled distal Ub (light blue) in a K27 diUb molecule shows displacement of some residues as quantified in Figure 3C.

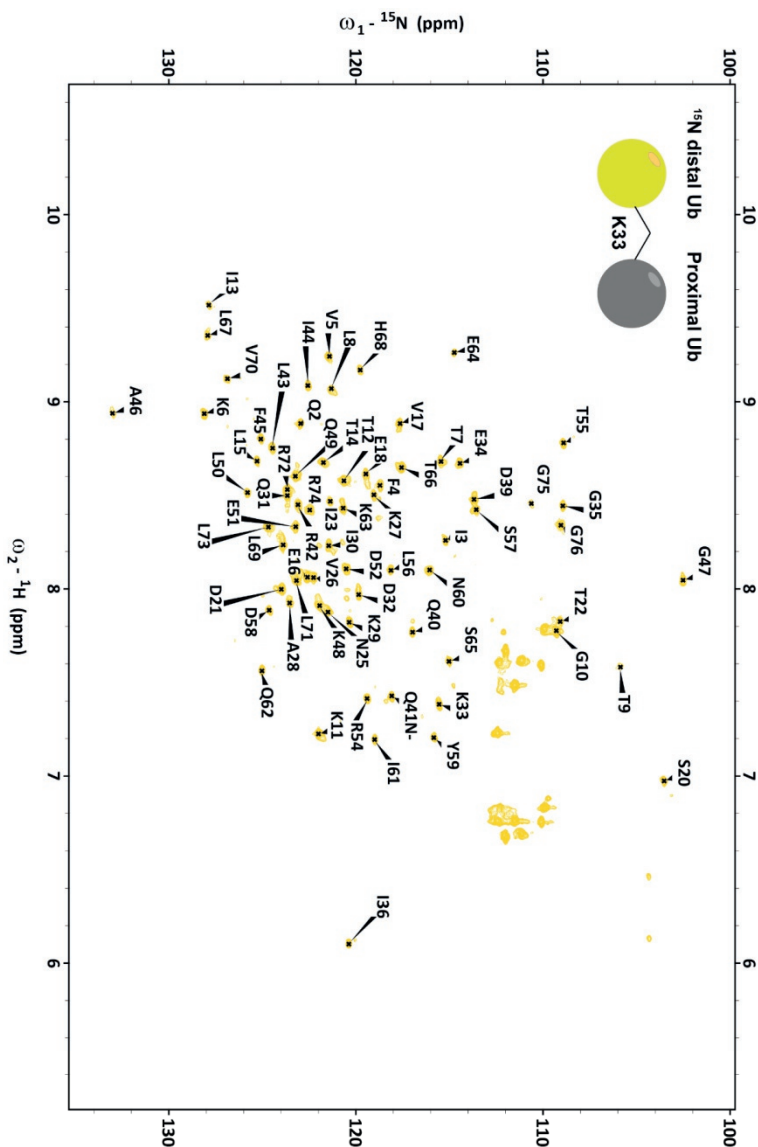


Figure S7: NMR spectrum of ^{15}N -Ub-K33-Ub (K33 diUb). The NMR (^1H - ^{15}N HSQC) spectrum of ^{15}N -labelled distal Ub (yellow) in a K33 diUb molecule shows displacement of some residues as quantified in Figure 3E.

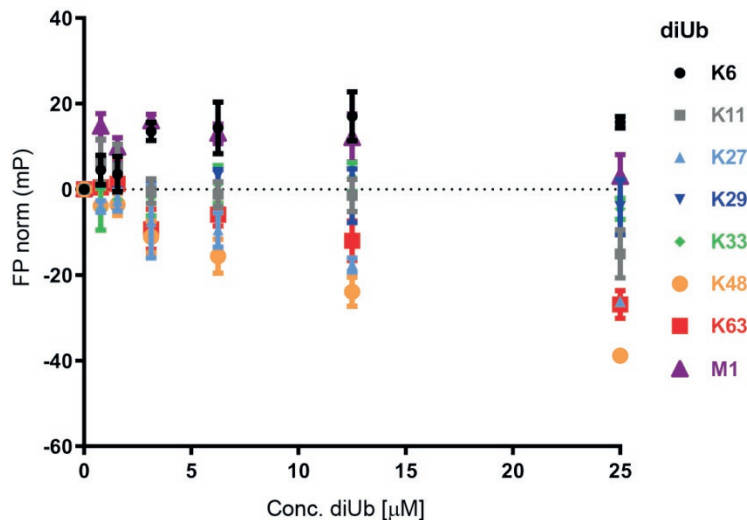


Figure S10: Fluorescence polarization assay using TAMRA-labeled UBXN1 UBA (1-42) domain and different concentrations of all 8 homotypical diUbs. There were no interactions of this binding domain with any of the diUbs tested.

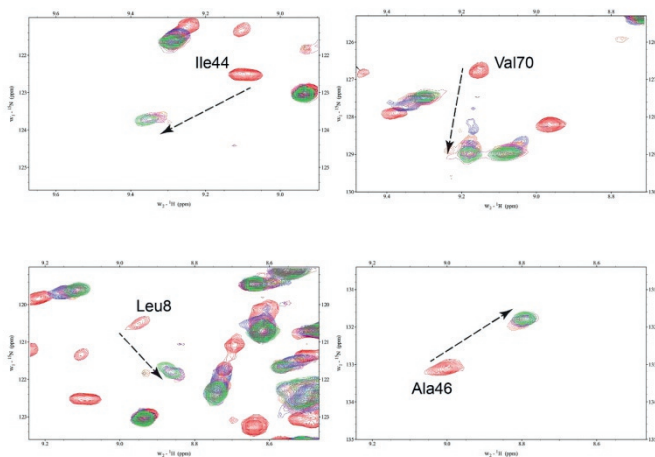


Figure S11: NMR spectrum showing key residues of the hydrophobic region in ^{15}N -Ub-K6-Ub (K6 diUb) added with different concentrations of unlabeled UBA(ext1-52) domain of UBXN1. Different colors represent the NMR (^1H - ^{15}N HSQC) spectrum of ^{15}N -labelled distal Ub in a K6 diUb molecule before (red) and after addition of 108 μM (blue), 135 μM (coral), 175 μM (purple), 270 μM (magenta) and 570 μM (green) of UBA domain.

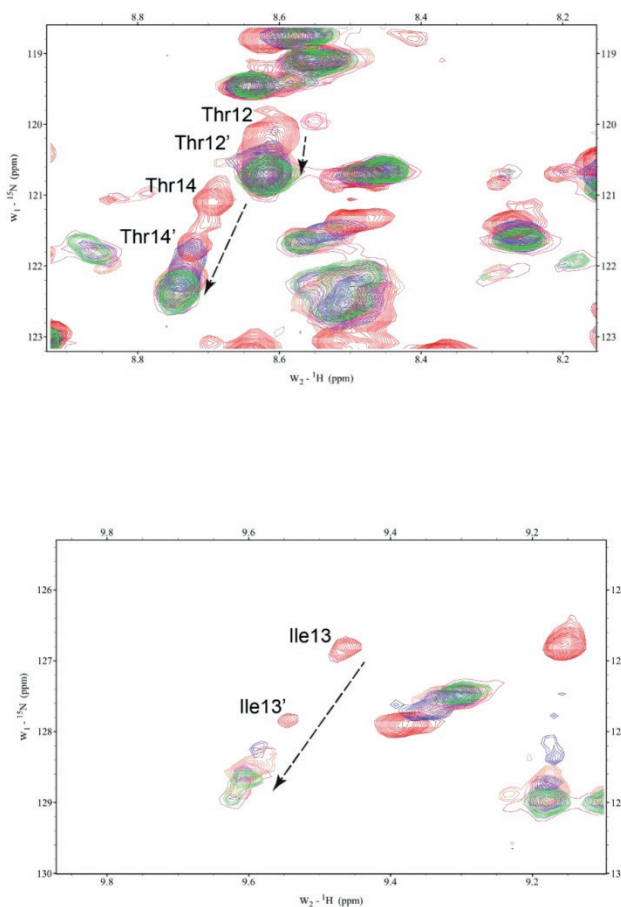


Figure S12: NMR spectrum showing Thr12, Thr14 (Top) and Ile13 (Bottom) signal shift in ^{15}N -Ub-K6-Ub (K6 diUb) added with different concentrations of unlabeled UBA(ext1-52) domain of UBAXN1. Different colors represent the NMR (^1H - ^{15}N HSQC) spectrum of ^{15}N -labelled distal Ub in a K6 diUb molecule before (red) and after addition of 108 μM (blue), 135 μM (coral), 175 μM (purple), 270 μM (magenta) and 570 μM (green) of UBA domain.

Diubiquitin-based NMR analysis

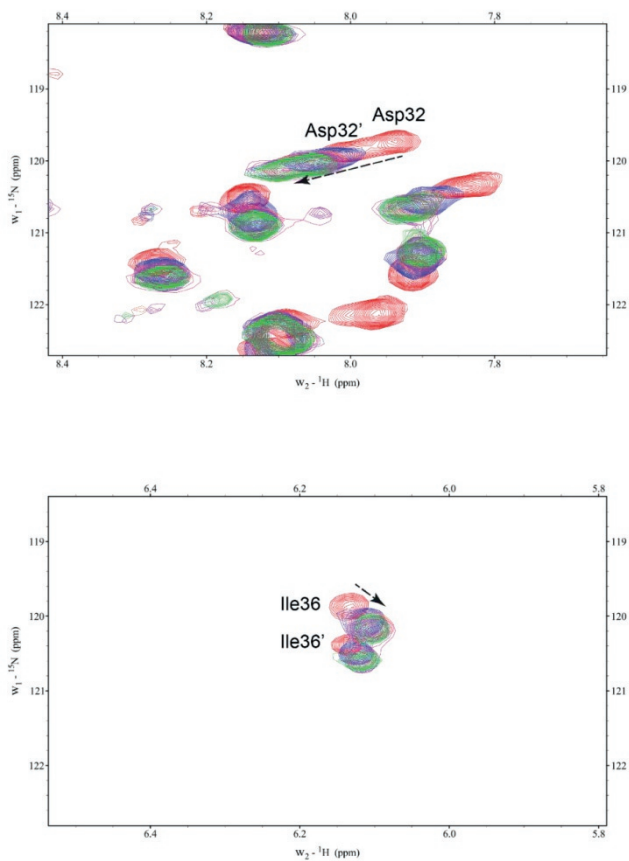


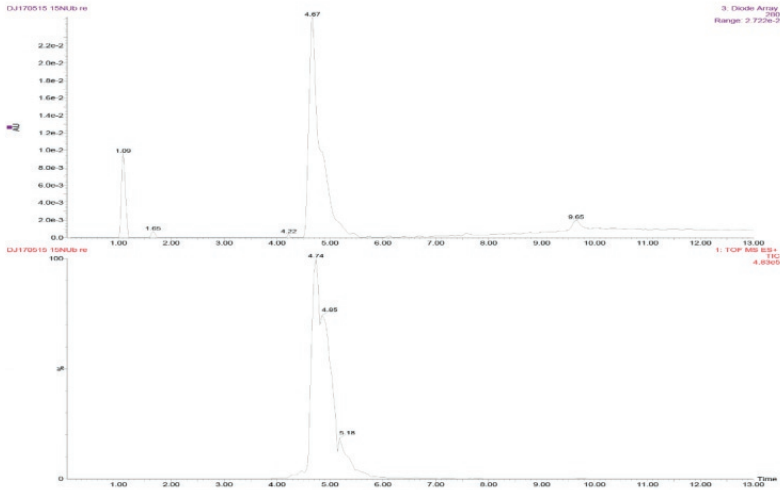
Figure S13: NMR spectrum showing split signals of Asp32 (Top) and Ile36 (Bottom) in ^{15}N -Ub-K6-Ub (K6 diUb) added with different concentrations of unlabeled UBA(ext1-52) domain of UBXN1. The NMR (^1H - ^{15}N HSQC) spectrum of ^{15}N -labelled distal Ub in a K6 diUb molecule before (red) and after addition of 108 μM (blue), 135 μM (coral), 175 μM (purple), 270 μM (magenta) and 570 μM (green) of UBA domain.

¹⁵N-Ub

¹⁵N-MQIFVKTLTGKTTITLEVEPSDTIENVKAKIQDKEGIPPDQQLIFAGKQLEDGRTLSDYNIQKESTLHLVLRLLGG

Calculated MW: 8670 Da
Observed MW: 8669 Da

A



B

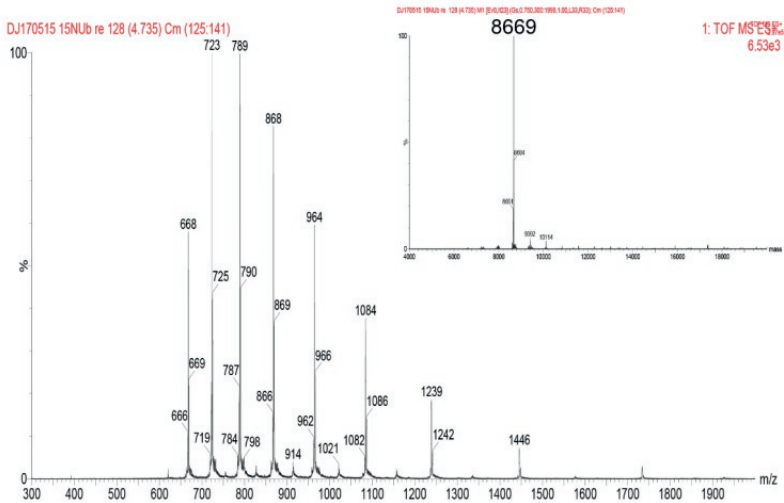


Figure S14: LC-MS analysis of ¹⁵N Ub sample. A. Top: UV chromatogram (λ – 280 nm); Bottom: Mass spectrum. B. Combined mass spectrum of peak at 4.67 min; Inset: Deconvoluted mass of mass spectra.

Diubiquitin-based NMR analysis

¹⁵N-Ub-K6Ub



Calculated MW: 17216 Da
Observed MW: 17212 Da

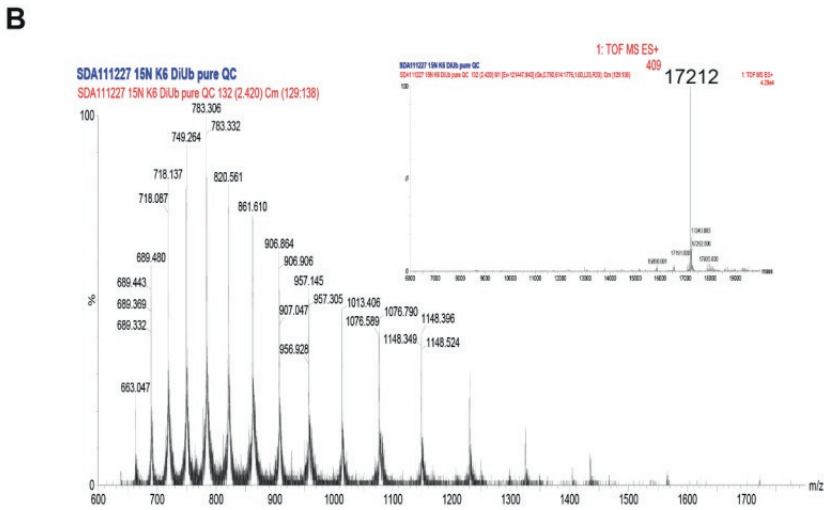
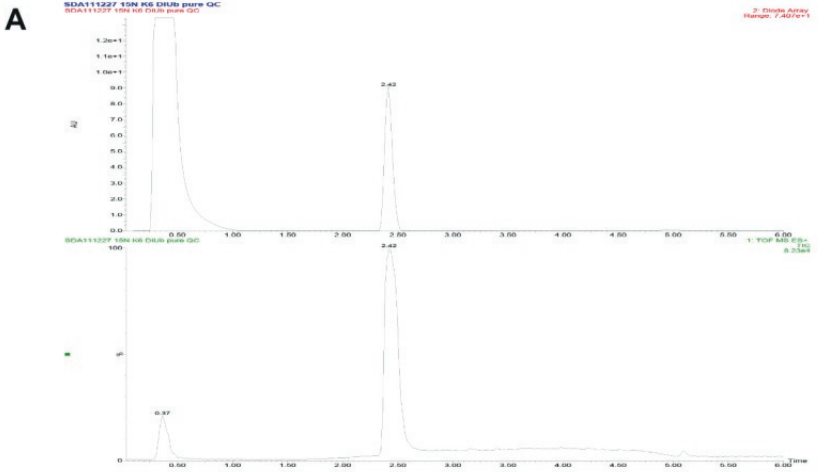


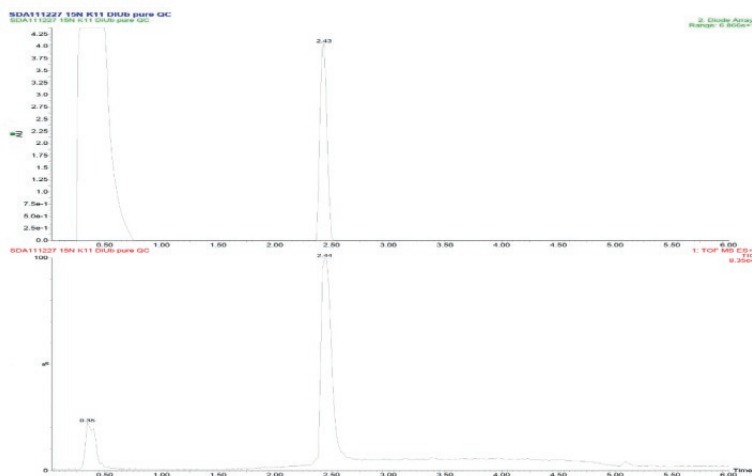
Figure S15: LC-MS analysis of ¹⁵N K6 diUb sample. A. Top: UV chromatogram (λ – 280 nm); Bottom: Mass spectrum. B. Combined mass spectrum of peak at 2.42 min; Inset: Deconvoluted mass of mass spectra.

¹⁵N-Ub-K11Ub

¹⁵N-MQIFVKTLTGKTTITLEVEPSDTIENVKAKIQDKEGIPPDQQRLLIFAGKQLEDGRTLSDYNIQKESTLHLVLRLRGG
 MQIFVKTLTGKTTITLEVEPSDTIENVKAKIQDKEGIPPDQQRLLIFAGKQLEDGRTLSDYNIQKESTLHLVLRLRGG

Calculated MW: 17216 Da
 Observed MW: 17212 Da

A



B

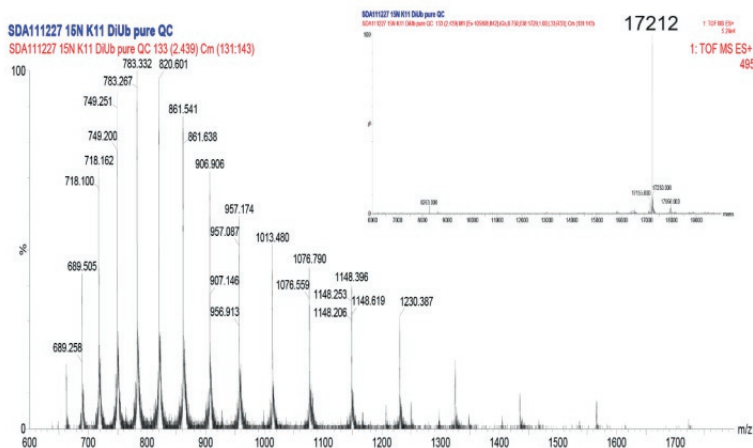


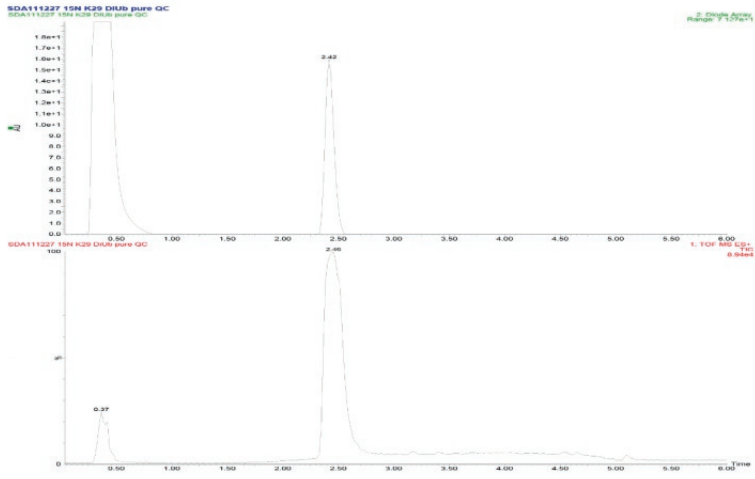
Figure S16: LC-MS analysis of ¹⁵N K11 diUb sample. **A.** Top: UV chromatogram (λ – 280 nm); Bottom: Mass spectrum. **B.** Combined mass spectrum of peak at 2.44 min; Inset: Deconvoluted mass of mass spectra.

¹⁵N-Ub-K29Ub

¹⁵N-MQIFVKTLTGKTTITLEVEPSDTIENVKAKIQDKEGIPPDQQLRFAGKQLEDGRTLSDYNIQKESTLHLVLRRLGG
 MQIFVKTLTGKTTITLEVEPSDTIENVKAKIQDKEGIPPDQQLRFAGKQLEDGRTLSDYNIQKESTLHLVLRRLGG

Calculated MW: 17216 Da
 Observed MW: 17212 Da

A



B

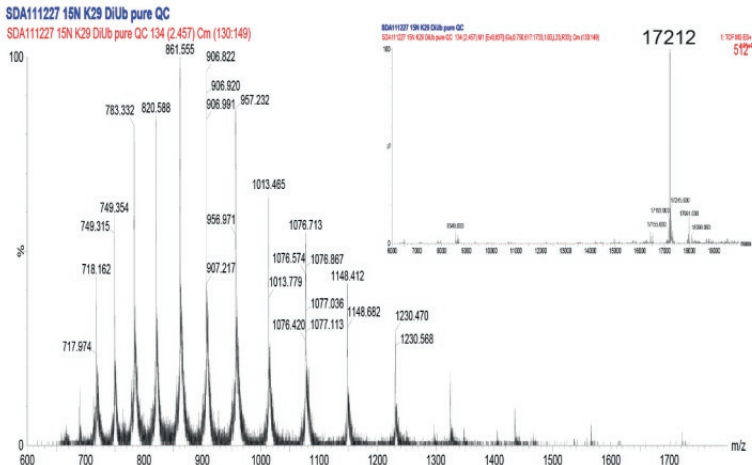


Figure S18: LC-MS analysis of ¹⁵N K29 diUb sample. A. Top: UV chromatogram (λ – 280 nm); Bottom: Mass Spectrum. B. Combined mass spectrum of peak at 2.46 min; Inset: Deconvoluted mass of mass spectra.

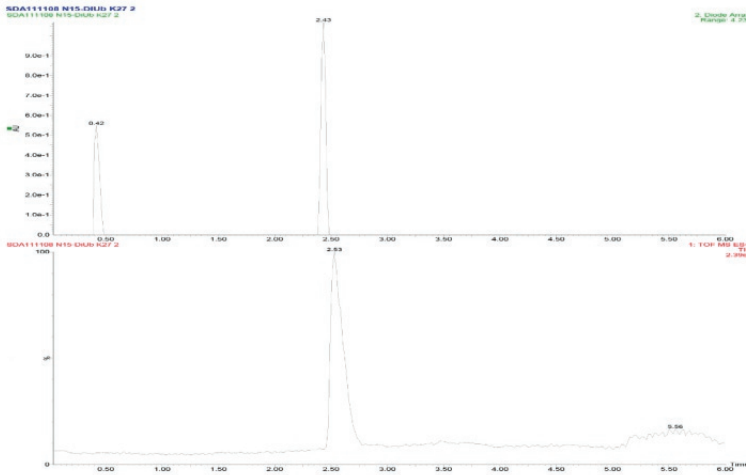
Diubiquitin-based NMR analysis

¹⁵N-Ub-K33Ub

¹⁵N-MQIFVKLTGKTTITLEVEPSDTIENVKAKIQDKEGIPPDQQRLLIFAGKQLEDGRTLSDYNIQKESTLHLVLRLLGG
 MQIFVKLTGKTTITLEVEPSDTIENVKAKIQDKEGIPPDQQRLLIFAGKQLEDGRTLSDYNIQKESTLHLVLRLLGG

Calculated MW: 17216 Da
 Observed MW: 17212 Da

A



B

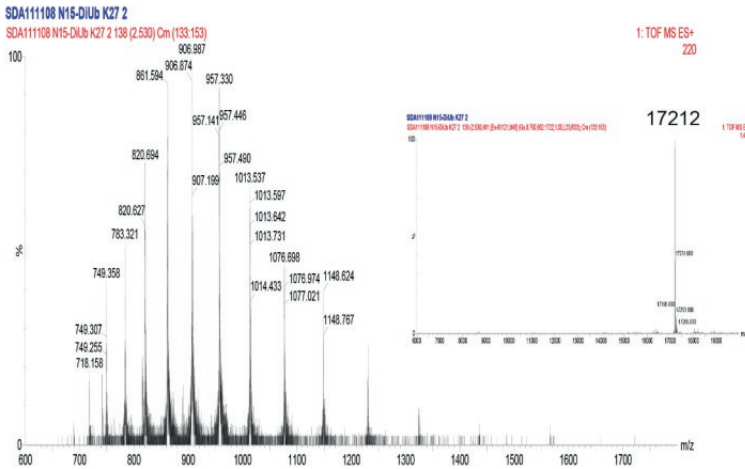


Figure S19: LC-MS analysis of ¹⁵N K33 diUb sample. A. Top: UV chromatogram ($\lambda = 280$ nm); Bottom: Mass spectrum. B. Combined mass spectrum of peak at 2.43 min; Inset: Deconvoluted mass of mass spectra.

¹⁵N-Ub-K48Ub

¹⁵N-MQIFVKLTGKTTITLEVEPSDTIENVKAKIQDKEGIPPDQQRLLIFAGKQLEDGRTLSDYNIQKESTLHLVLRRLGG
 MQIFVKLTGKTTITLEVEPSDTIENVKAKIQDKEGIPPDQQRLLIFAGKQLEDGRTLSDYNIQKESTLHLVLRRLGG

Calculated MW: 17216 Da
 Observed MW: 17212 Da

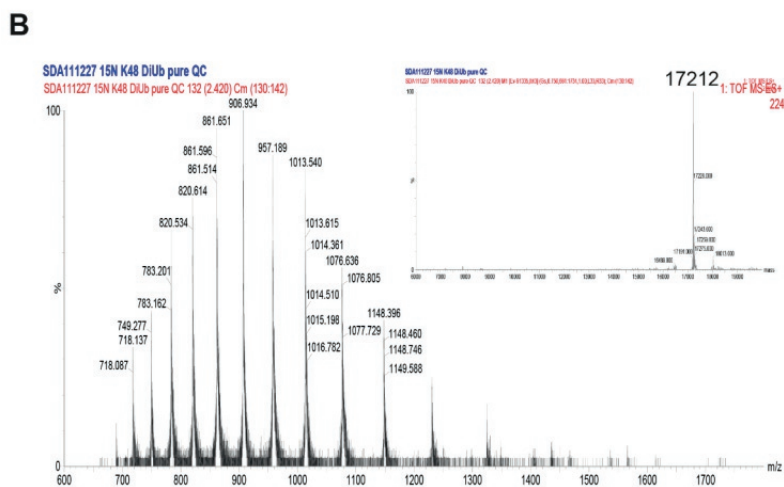
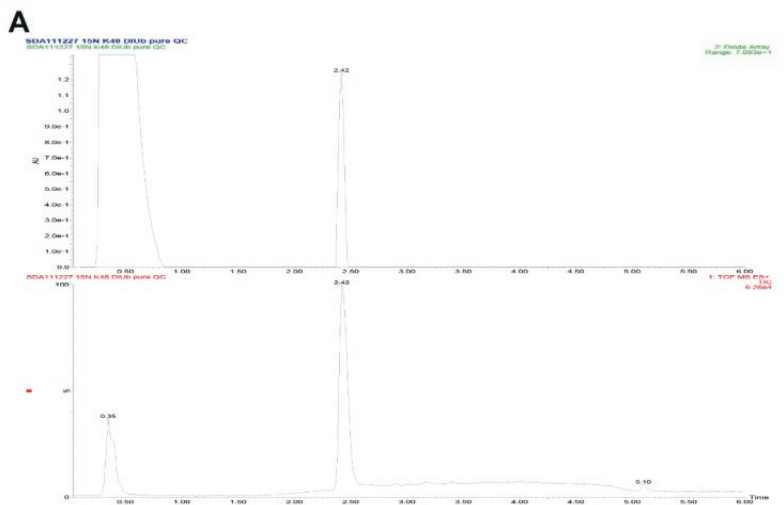


Figure S20: LC-MS analysis of ¹⁵N K48 diUb sample. A. Top: UV chromatogram (λ – 280 nm); Bottom: Mass spectrum. B. Combined mass spectrum of peak at 2.42 min; Inset: Deconvoluted mass of mass spectra.

Diubiquitin-based NMR analysis

¹⁵N-Ub-K63Ub

¹⁵N-MQIFVKTLTGKTTITLEVEPSDTIENVKAKIQDKEGIPPDQQRLLIFAGKQLEDGRTLSDYNIQKESTLHLVLRLLGG
 MQIFVKTLTGKTTITLEVEPSDTIENVKAKIQDKEGIPPDQQRLLIFAGKQLEDGRTLSDYNIQKESTLHLVLRLLGG

Calculated MW: 17216 Da
 Observed MW: 17212 Da

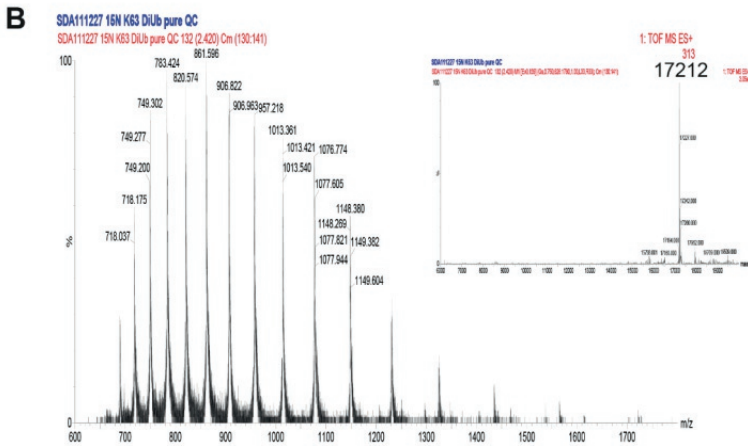
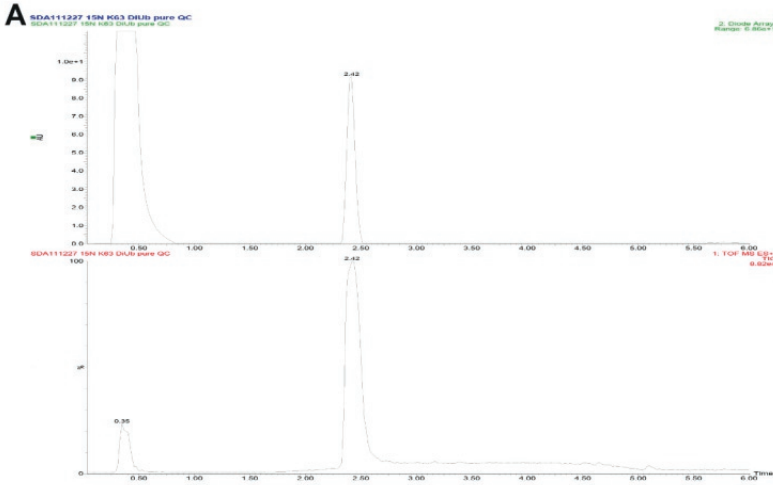


Figure S21: LC-MS analysis of ¹⁵N K63 diUb sample. A. Top: UV chromatogram (λ – 280 nm); Bottom: Mass spectrum. B. Combined mass spectrum of peak at 2.42 min; Inset: Deconvoluted mass of mass spectra.